INSTITUTO SUPERIOR TÉCNICO
Universidade Técnica de Lisboa

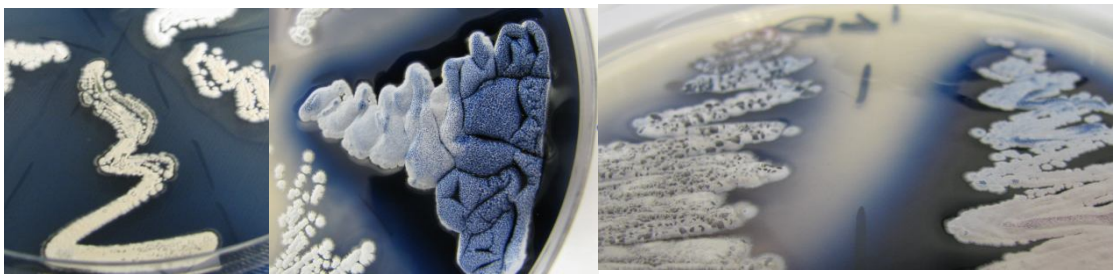

The Phosphoenol-Pyruvate-Oxaloacetate node in *Streptomycetes*: a study on pyruvate carboxylase

João Carlos Santos Cruz

Dissertation for the Master's Degree in

Biological Engineering

Jury

President: Professor Doutor Duarte Miguel de França Teixeira dos Prazeres, Departamento de Bioengenharia (DBE)

Supervisor: Professor Doutor Nuno Gonçalo Pereira Mira, Departamento de Bioengenharia (DBE)

Doutor Paul A. Hoskisson, University of Strathclyde, Glasgow, UK

Arguer: Professor Doutor Miguel Nobre Parreira Cacho Teixeira Departamento de Bioengenharia (DBE)

September 2012

Acknowledgments

I would like to thank Professor Paul Hoskisson Research group, especially to Jana Hiltner, whose experience and patience steered me throughout this project. It is also important to mention the support and guidance provided by Prof. Paul Hoskisson and Prof. Nuno Gonçalo Pereira Mira.

Completing this chapter of my life would not have been possible without the support of my family and friends. I huge thanks to Pico, Márcia, Simão, Pedro, Tiago, Sara and Joana, for bearing with me on all the study sessions and group works and also to my parents and sister who have always gave me nothing but support and confidence.

Resumo

Neste trabalho foi estudado o papel do nó Phosphoenolpiruvato-Piruvato-Oxaloacetato no crescimento, atividade metabólica e na produção de Actinorodina e Undecilprodegiosina por *Streptomycetes* um dos géneros mais usado para a produção de antibióticos. Este trabalho foca-se na carboxilação do piruvato pela enzima piruvato carboxilase, a qual tem um papel crucial nas reações anapleróticas de *S. coelicolor.*

De forma a efetuar a análise funcional da enzima PCx em *S. coelicolor,* o gene que codifica esta enzima foi eliminado usando uma estratégia de eliminação baseada no uso de transposões. Entre outros resultados, a eliminação do gene que codifica a enzima PCx em *S. coelicolor* dirigiu o fluxo de carbono para uma maior produção de acetil-CoA o que conduziu a um aumento da quantidade de actinorrodina quando comparado com os níveis produzidos pela estirpe parental.

Foi também feita uma análise *in silico* dos domínios previstos para esta enzima. Os resultados obtidos mostram uma elevada conservação da enzima PCx *S. coelicolor* com o de outras enzimas indicando que o mecanismo de catálise e regulação envolvido é, presumivelmente, similar com o de outros organismos. Na caracterização bioquímica da enzima PCx foi possível concluir que os domínios similares à síntese da molécula carbamoil-fosfato e à transferência do grupo carboxil através da biotina são essenciais à atividade da proteína.

Espera-se que os resultados deste trabalho possam contribuir para um conhecimento mais aprofundando do papel do nó Phosphoenolpiruvato-Piruvato-Oxaloacetato na atividade metabólica de *S. coelicolor*, o que pode ser usado na manipulação genética com vista ao aumento da produção de antibióticos.

Palavras-chave Nó fosfoenolpiruvato-piruvato-oxaloacetato; Piruvato carboxylase; *Streptomyces coelicolor* A3(2); Anaplerosis; Actinorodina

Abstract

This work was dedicated to the study of the Phosphoenolpyruvate-Pyruvate-Oxaloacetate node in *Streptomyces coelicolor*, a natural produced of Actinorhodin and Undecylprodegiosin and an important genus in antibiotic production. In particular, it was examined the effect in normal carbon flux and anaplerotic functions during antibiotic production. This node is a major control point of carbon flux providing precursor molecules for several biosynthesis pathways.

To perform a functional analysis of PCx enzyme in *S. coelicolor*, the encoding gene was eliminated using a transposon mutagenesis strategy. Among other results it possible to verify that this elimination directed the carbon flux into Acetyl-CoA leading to an increase of Actinorhodin.

The *in sillico* analysis of the predicted domains of this enzyme show an elevated conservation of PCx enzyme indicating that catalysis and regulation mechanisms should be similar to other organisms. From the biochemical characterisation of the enzyme it was possible to conclude that the carbamoyl phosphate synthase and biotin carboxylase carrier domain are indispensable to the protein activity.

It is expected that the results of this work may contribute to a deeper knowledge of the phosphoenolpyruvate-pyruvate-oxaloacetate-node's role in *S. coelicolor* metabolic activity. Knowledge that could be used to genetic manipulate this microbe in order to obtain a higher antibiotic production.

Key Words: Phosphoenolpyruvate-Pyruvate-Oxaloacetate node; Pyruvate Carboxylase; *Streptomyces coelicolor* A3(2); Anaplerosis; Actinorhodin

Index

Figure Index

Table Index

Glossary

PEP – Phosphoenolpyruvate

PYR – Pyruvate

OAA – Oxaloacetate

PCx – Pyruvate Carboxylase

Alcan – N-Acetylglucosamine

Act – Actinorhodin

PKS – Polyketide Synthase

ATP – Adenosine Triphosphate

TCA – Tricarboxylic Acid

PPP – Pentose Phosphate Pathway

Kan^R – Resistance cassette to Kanamycin antibiotic

Apr^R – Resistance cassette to Apramycin antibiotic

Amp^R – Resistance cassette to Ampicillin antibiotic

Tst^R – Resistance cassette to Thiostrepton antibiotic

CHL – Chloramphenicol

SDS-PAGE – Sodium Docedyl Polyacrylamide Gel Alectrophpresis

HMGL - Hydroxymethyl Glutaryl-Coa Lyase

1. Introduction

By the end of the first half of 20th century, antibiotics held a great premise regarding the eradication of infections as major health threat. However these past few years have proven that a war against infectious agents is far from over, showing that investment in this area should not be disregarded as the antibiotic resistance rises giving origin to many multi-drug resistant strains [1].

One major contributor for the production of known antibiotics of microbial origin is the member of the Actinomycetales, which includes the *Streptomyces* genus. Bacteria of this genus are responsible for approximately two thirds of the identified antibiotics from microbial origin, which translates into over 6000 different molecules produced by these bacteria including streptomycin or chloramphenicol. Despite their already significant contribution for antibiotic production, these bacteria are still considered interesting candidates for drug discovery [2-4].

The organism used in this study is *S. coelicolor* A3(2). Although it is a well- studied strain and is often used as a model organism for *Streptomyces*, its metabolism is not yet fully understood, a knowledge that is crucial to enhance yield of antibiotics produced in this bacteria and that can also contribute for the discovery of novel molecules [5].

Having in mind that the most interesting compounds are produced as secondary metabolites, it is important to understand what can be done to enhance the production of such substances [6]. One of the gaps that has not been studied to its full extent is the Phosphoenolpyruvate-Pyruvate-Oxaloacetate (PEP-PYR-OAA) node. This node can be seen as the metabolic link between glycolysis, gluconeogenesis and the tricarboxylic acid cycle (TCA), as well as for other secondary metabolic pathways including the Polyketide Synthase (PKS) System. This node plays a crucial role in controlling carbon flux according to the microorganism needs and thus its manipulation can result in the alteration of different metabolic routes including those that can lead to increased antibiotic production [7].

From all the metabolic steps that characterise the node, the conversion of pyruvate into oxaloacetate by pyruvate carboxylase enzyme was under special scrutiny in this work. The results obtained could be important to better understand the consequences that a blockage of this metabolic route could have in antibiotic production driven by this bacteria [8].

2. Literature Review

Although several antibiotics have been discovered over the last 50 years with its peak in the 60s, the overuse of those drugs has led to an increasing antimicrobial resistance and such fact raises some attention regarding human healthcare. The upsurge of multiple antibiotic resistant agents implies that the policies regarding this problem have to be reviewed, namely those involving the overuse of such drugs. Nevertheless a strong investment in research for new and enhanced antibiotics is also vital [9].

The main goal of this project was to supply more information on a critical metabolic node of a known antibiotic producer and to see what could be done with such knowledge to improve the currently achieved yields of antibiotic production.

Different schemes are used to group or classify antibiotics but one that is relatively efficient is to group these molecules according to their chemical structure, a classification that allows clustering the antibiotics having similar properties in terms of effectiveness, toxicity, and allergic potential. *Streptomyces coelicolor* A3(2) is a natural producer of actinorhodin (a benzoisochromanequinone)[10], undecylprodigiosin (a tripirrole) [11], methylenomycin (a cyclopentanone) [12], and calcium-dependent antibiotic (acidic lipopeptide) [13].

2.1. *Streptomyces coelicolor* A3 (2) - a systems model

One of the largest phyla of the domain Bacteria are actinobacteria (also known as Actinomycetes) which includes the genus *Streptomyces*. Actinobacteria can be found in different shapes ranging from coccoid (Micrococcus) shape to highly differentiated branched mycelium (*Streptomyces*), but the diversity does not limit itself to morphological differences, these organisms can be found in diverse habitats and show varied physiological and metabolic properties such as the production of extracellular enzymes and the formation of secondary metabolites, and such metabolites can present as potent antibiotics, immunosupressors or anti-cancer drugs [14].

This work will focus on *Streptomyces spp*, although there was some confusion regarding its taxonomic position in the past, it is now proven that *Streptomyces* is a bacterium and belongs to the phylum Actinobacteria. However, the fact that it is so different from the regular rod-shaped bacteria that were usually studied, at first, raised some doubts about this organism's claim to be seen as bacteria. Nevertheless the fact that lacks nuclear membrane, presents a cell-wall structure as usual in Gram-positive bacteria and has some sensibility to anti-bacterial antibiotics constituted enough evidence of the right taxonomic position of this organism [15].

The strain used in this project was *Streptomyces coelicolor* A3(2), a saprophytic soil bacterium that obtains nutrients and energy by degrading insoluble organic materials (e.g.

chitin, xylan, and cellulose) through the production of a variety of extracellular hydrolytic enzymes [16, 17]. This species has been under the scope of microbiologists for more than 50 years due to their potential in antibiotic production. However, guaranteeing a reproducible growth of the filamentous species has been a challenge and the optimization of industrial conditions to produce a reproducible quantity of antibiotics on each fermentation has been a major hurdle[18]

The S. coelicolor genome has been sequenced in 2002 which offers a great advantage to the understanding of its metabolic activity and involvement in the production of bioactive molecules. In a universe of more than 8.5Mbp, 7,825 predicted genes (including over 20 clusters of genes responsible for producing secondary metabolites) have been identified [19].

One of the most distinctive features of microbes of *S. coelicolor* is their life cycle. *Streptomyces* exhibits a complex developmental cycle involving a set of physiologically distinct stages including sporulation, spore germination, vegetative hyphal growth or the production of aerial hyphae [20]. Growth occurs through tip extension with the initiation of new branches, and consequently, the new cell-wall material synthesis only at happens the hyphal tips [21].

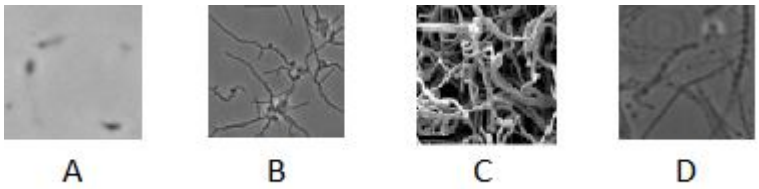

Figure 2.1 - Different stages of Streptomyces life cycle. A-Spore germination[this work]; B – Vegetative mycelia[this work]; C- Aerial hyphae [22]; D – Spore formation [this work]

In Figure 2.1 it is possible to identify the different stages of *S. coelicolor* life cycle. Image A shows a spore germinating, where it can be identified a spore and small branch, while in image B the formation of the vegetative mycelia starting to entangle with other spores branches can be seen. In imagine C it is depicted the aerial hyphae, a fluffy white aerial mycelium which may contain over 50 copies of the genome in the hyphae tips that will eventually go into multiple cell division closing the cycle with spore formation (represented in image D).

It is important to highlight that the aerial hyphae are only formed under specific conditions of humidity or nutrient availability[6, 23]. In fact, even the spores present different properties when the sporulation process happens in submerged cultures or in solid media. In the case of *Streptomyces coelicolor* no spores are formed in liquid media, which may indicate a significant difference in the organisms metabolism [24].

Still *S. coelicolor* presents a biphasic growth pattern with an initial exponential phase followed by a slower stage of biomass increment. Antibiotic production happens mostly during the stationary phase, when growth is arrested [25, 26]. In the study of Bibb (2005) it is

demonstrated that the antibiotic production, in liquid-grown cultures, is generally confined to stationary phase, assumed to result from nutrient limitation. In the same work, also it has also been demonstrated that the regulation of secondary metabolism in streptomycetes is distinctively diverse and complex, which may have an impact in the activity of metabolic routes leading to antibiotic production [27]. Extracellular environmental signals and nutrient limitation signals are transduced through global regulators that may activate different pathway specific regulators and influence antibiotic production [28, 29]. An example of this are the *bld* genes which are required for aerial hyphae or spore formation and that also influence antibiotic production [30].

Besides its involvement in carbon and nitrogen metabolism, GlcNac is also an important signalling molecule for streptomycetes and a major decision point toward the onset of development and antibiotic production.[29]

Figure 2.2 presents a good example of the complexity inherent to the antibiotic production introducing some of the factors mentioned earlier plus some others as the highly phosphorylated guanine nucleotides (ppGpp) which has been proved to be implicated in microbial growth and having an influence on antibiotic production[31].

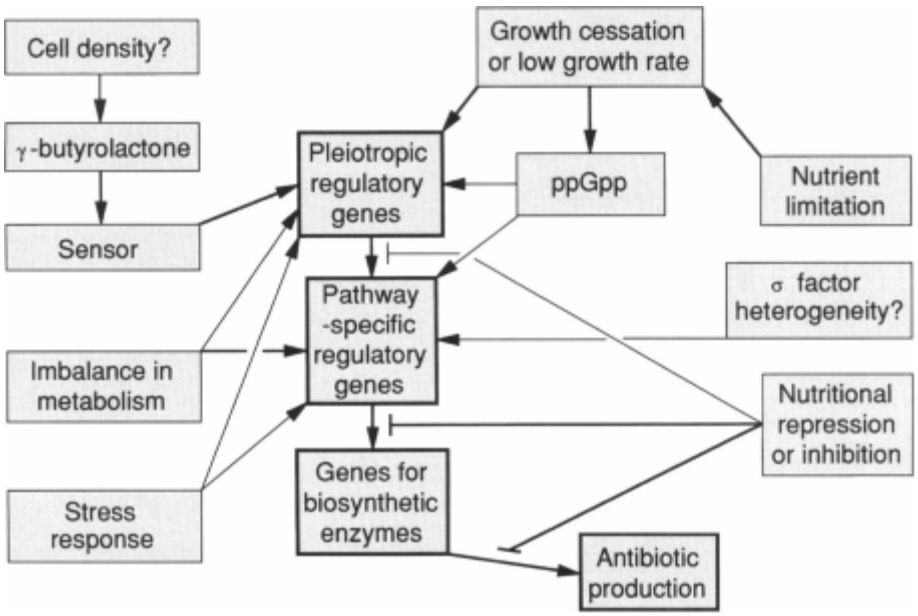

Figure 2.2 - Scheme of the different factors influencing antibiotic production. Adapted from Bibb 1996 [32]

Although *Streptomyces coelicolor* A3(2) produces different antibiotics this work is only focused to the production of actinorhodin and undecylprodigiosin, two antibiotics belonging to the family of polyketides and pyrrolic compounds, respectively. The production of actinorhodin itself is not interesting from a pharmaceutical point of view as it is an antibiotic with low activity[33], however as a polyketide molecule its synthesis is similar to other more active molecules from this family [34].

Nieselt et al. 2010 [25], while studying the metabolic switch, showed how actinorhodin and undecylprodigiosin start to be produced when the biomass growth stabilizes just as it is represented on Figure 1.4.

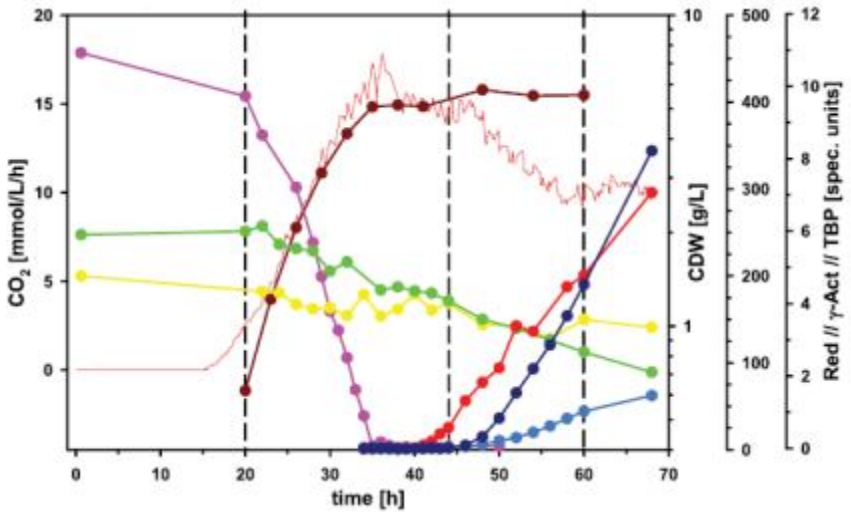

Figure 2.3 - Example of a *S. coelicolor* A3(2) growth curve and production of Actinorhodin, and undecylprodegiosin as phosphate, glucose and glutamate depletion. Increase in biomass (brown), phosphate depletion (pink), the decrease of glucose (yellow) and glutamate (green) levels, as well as the production of the antibiotics undecylprodigiosin (red), actinorhodin (blue), and total blue pigment (light blue). Continuous measurements of CO_2 production are indicated by the thin red line.[25]

As it is noted in this figure both undecylprodigiosin and actinorhodin are produced during stationary phase, with undecylprodigiosin biosynthesis being the first to be produced. Although it is not important for this work to make a very thorough analysis of the antibiotic biosynthesis, mentioning some of the molecules involved in these reactions will be important to achieve a better understanding of what to expect from this work. During growth of *S. coelicolor* A3(2) in solid media the colonies can acquire different colours depending on the antibiotic they are producing: a red pigmentation is due to the production of pyrrole based antibiotics, namely undecylprodigiosin, while the blue pigmentation is associated to the production of actinorhodin .

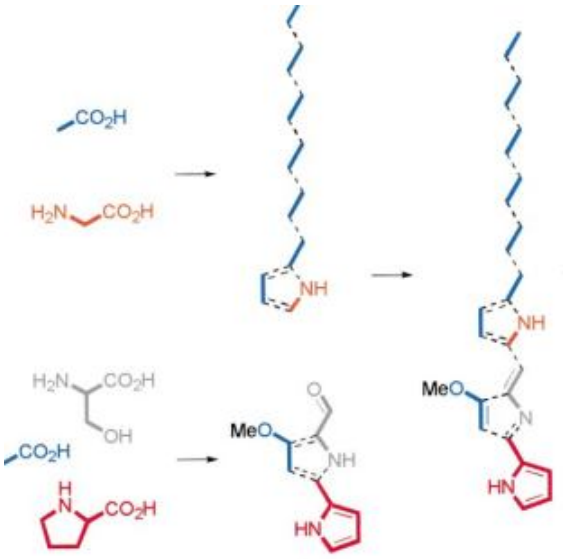

Figure 2.4 - The biosynthetic origin of undecylprodigiosin Acetate -Blue; Serine – Grey; Proline – Red; Glycine – Orange; Adapted from Cerdeño et al.[35]

Figure 2.4 shows the biosynthetic pathway leading to the production of Undecylprodegiosin. This picture shows that production of undecylprodegiosin requires one unit of proline, one unit of glycine, one unit of serine and several units of acetate.

On the other hand, actinorhodin belongs to a class of aromatic polyketides, the benzoisochromanequinone antibiotics. In fact, this antibiotic played a vital role on understanding type II polyketide synthase (PKS) system.

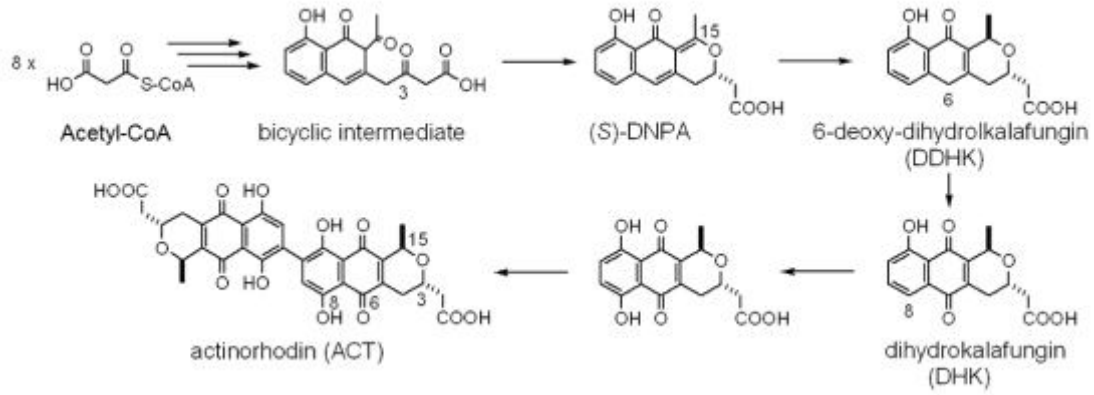

Figure 2.5 - The biosynthetic origin of actinorhodin. Adapted from Okamoto et al.[10]

On Figure 2.5 it is explained a very simplified scheme of actinorhodin biosynthesis, as it does not describes all the condensation reactions that characterize the poliketyde synthase system[36], showing only the molecule of acetyl-CoA as a starter for this reaction and some of

the intermediates between that molecule and actinorhodin. Below these pathways will be analysed in more detail.

2.2. The polyketide synthase system and the glyoxylate shunt

This topic is dedicated to two pathways relevant for the execution of this project: the polyketide synthase system and the glyoxylate shunt. Biosynthesis of polyketides is thought to have evolved from fatty acid biosynthesis. The carbon backbone of a polyketide results from a sequential condensation of several C2-molecules like acetate or acetyl-CoA. There are two types of enzymes complexes catalyzing the synthesis of polyketide backbones enzyme complex I and II, although in this work only on the set of enzymes that compose type II [34, 37, 38].

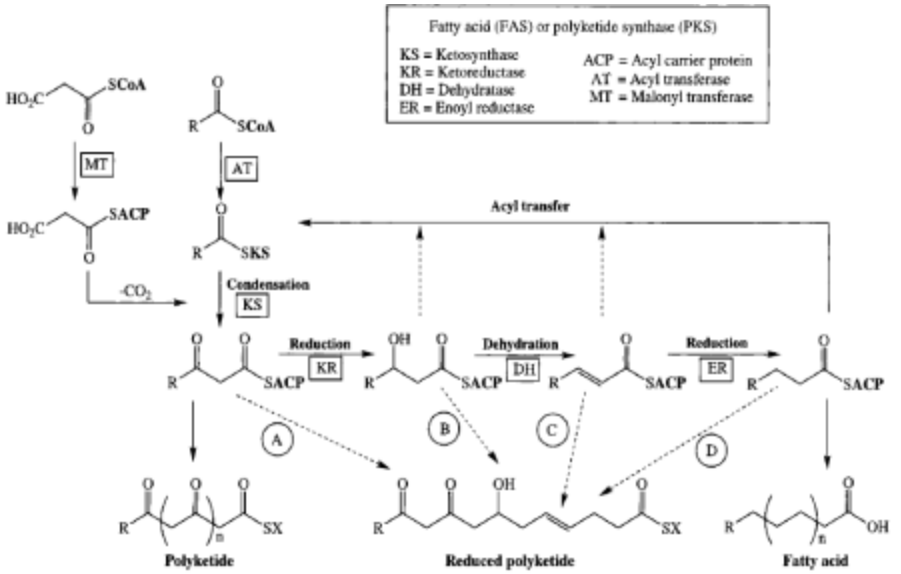

Figure 2. 6 – Fatty acid and polyketide synthesis simplified reaction scheme [34]

Figure 2.6 describes, in a simplified scheme, the biosynthesis of the polyketides. Two facts should be highlighted: i) the starter molecule, acetyl-CoA, establishes a link between common metabolic pathways used in central carbon metabolism; ii) the similarities between PKS system and fatty acids synthases (FAS) system which were important to achieve a better understanding of this system (a more detailed pathway is available on Annex Chapter, Annex Figure Ia and Ib).

The glyoxylate shunt can be seen as a shortcut “inside” the TCA cycle, requiring acetyl-CoA and transforming it in succinate. This pathway offers the possibility to use smaller carbon compounds as sole carbon source (e.g. acetate) and create some of the intermediates of the TCA cycle replenishing it with some molecules that are usually obtain using molecules with a longer carbon backbone[39].

2.3. The Phosphoenolpyruvate-Pyruvate-Oxaloacetate Node

This node can be seen as the metabolic link between three main pathways of central carbon metabolism: glycolysis, gluconeogenesis and the TCA Cycle, pyruvate being the molecule that interconnects these three metabolic routes. As the name implies this node regulates the interconversion of pyruvate, phosphoenopyruvate, and oxaloacetate but also acetyl-CoA, acetate, and malate [7]. This node has a vital role in the control of the microorganism development considering its involvement in the control of carbon fluxes inducing a catabolic metabolism or an anabolic one, depending on the environmental conditions[7]. Consistently, some of the enzymes of the node may be essential for growth under given conditions. For instance, in *B. subtillis* pyruvate carboxylase is indispensable when cells are growing using carbohydrates as the sole carbon sources [40-43].

Figure 2.7 resumes all the reactions of this node, showing the anaplerotic functions and their connection with the other pathways. In this picture is possible to see how this node can initiate gluconeogenesis (by adding a carboxyl group to a pyruvate molecule transforming it into oxaloacetate and from that forming PEP until it reaches glucose) or how it can supply the TCA cycle (by forming malate, oxaloacetate and acetyl-CoA) and also how it depends on glycolysis to the formation of pyruvate. One of the most significant roles of the PEP-PYR-OAA node is its anaplerotic function towards the TCA cycle. For example, pyruvate carboxylase provides the Krebs cycle with oxaloacetate from the carboxylation of pyruvate [43, 44].

One interesting feature of this node is the fact that it also has the precursors for the antibiotic biosynthesis which could open another door towards improving antibiotic production.

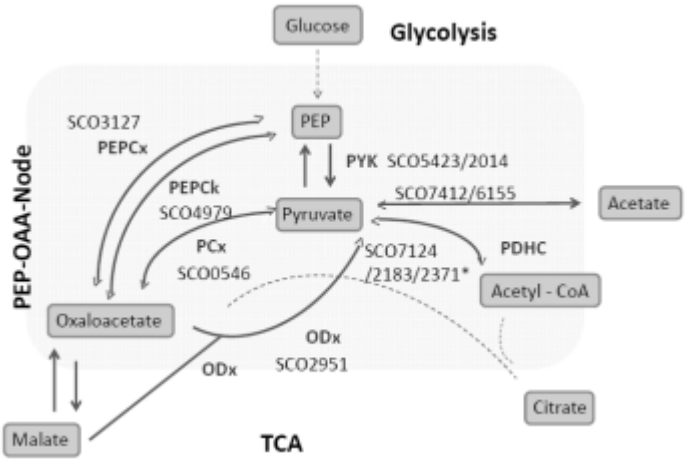

Figure 2.7 - Phosphoenolpyruvate-Pyruvate-oxaloacetate Node reactions scheme in *S. coelicolor*. (Figure kindly provided from J. Hiltner [27])

The formation of undecylprodigiosin requires proline, glycine and serine[35] Some of these molecules directly produced from pyruvate thus turning their biosynthesis sensible to a PEP-PYR-OAA node regulation.[45] On the other hand actinorhodin, as a polyketide antibiotic, needs acetyl-CoA as a starter molecule to its biosynthesis, which renders it PEP-PYR-OAA node dependent as well. Therefore the manipulation of this node can be an efficient way to improve the production of both antibiotics, actinorhodin and undecylprodigiosin.

Studies have been demonstrating that the regulation of this node is more complex and goes beyond than a simple On/Off regulation system. It has been found that more than one of the enzymes of the node may be active at the same time. Furthermore, one enzyme may fulfil different functions with the same reaction, which has been posing a serious barrier to the full elucidation of the PEP-PYR-OAA node [46].

One solution to partially resolve this problem is to characterise every reaction independently and later on to conjugate all the knowledge obtained this way. For this project this was the line of thinking followed, therefore the conversion of pyruvate into oxaloacetate was studied in more detail.

2.4. The pyruvate carboxylase enzyme

This work has examined in more detail the reaction of the PEP-PYR-OAA node catalysed by the pyruvate carboxylase enzyme.

Pyruvate carboxylase activity was described for the first time by Utter and Keech [47] and it has been discovered across vertebrates, invertebrates and microorganisms. In general, by adding a carboxyl group into a pyruvate to form an oxaloacetate molecule (see reaction 1), PCx can provide an intermediate to Krebs cycle or initiate the gluconeogenesis pathway.

Although pyruvate carboxylase plays a major anaplerotic role, only few prokaryotes use it as the sole anaplerotic enzyme [7].The other possible route for oxaloacetate synthesis are carboxylation of phosphoenolpyruvate (PEP) by its carboxylase which in many organisms replaces completely PCx, hence it cannot be find naturally in Enterobacteria, for instance.[48, 49]. However, due to the importance of the anaplerotic functions, some microorganisms may hold more than one enzyme to accomplish the same goal, possessing both, a PEP carboxylase and a PCx as anaplerotic enzymes[43]. Indeed, March et al. (2002) have proven that providing PCx to *E. coli* (which has only PEP carboxylase) augments cell growth presumably because it turns glucose catabolism more efficient [49].

Oxaloacetate plays a very important role in the cell metabolism being not only an intermediate on TCA cycle but also a precursor for biosynthesis of several amino acids including aspartate, methionine and lysine. Oxaloacetate is also a precursor for biosynthesis of

pyrimidines. The continuous removal of oxaloacetate during the growth of microorganism is thus expected making the replenishment of this molecule crucial[39].

Anaplerotic reactions are very important to replenish the TCA cycle and pyruvate carboxylase (PCx) is considered one of the main anaplerotic enzymes[44]. For instance, in *Saccharomyces cerevisiae*, the two main pathways to replenish the TCA cycle with oxaloacetate are *via* the carboxylation of pyruvate by PCx and from the glyoxylate shunt, this later is being repressed during growth on glucose leaving PCx as the only known enzyme with the ability to replenish the Krebs cycle with oxaloacetate [50]. In mammals, the role of PCx enzyme varies with its location: in liver and kidney the primary role of PCx is to participate in gluconeogenesis, while in adipose tissue it contributes to the synthesis of NADPH which is required for lipogenesis. PCx was also found in plants providing an alternative gluconeogenic pathway to the photosynthetic process during germination [51].

The ATP-dependent carboxylation catalyzed by PCx is a two step reaction. As it is demonstrated on reaction 1 PCx belongs to a large family of biotinylated enzymes that carry out carboxyl group transfer in a variety of reactions. These enzymes use biotin to transfer the carboxyl group between active sites.

$$Enzyme - Biotin + ATP + HCO_3 \longrightarrow Enzyme - Biotin - CO_2 + ADP + P_i \quad (1)$$

$$Enzyme - Biotin - CO_2 + Pyruvate \longrightarrow Oxaloacetate + Enzyme - Biotin \quad (2)$$

Pyruvate does not contain a high-energy phosphate bond or favourable thermodynamics, thus, it is required to acoplate the catabolism of an ATP molecule for the reaction to proceed. The first partial reaction is the biotin carboxylation and it is described as a two-step procedure starting with activation of the bicarbonate with ATP followed by the carboxylation of the biotin with the recently formed carboxyphosphate. The second partial reaction involves the transfer of the carboxyl group into the pyruvate molecule forming oxaloacetate (a complete mechanism of this reaction is available in Annex Figure II) [52, 53].

In this last section it is carried an overview of PCx structure. It has been found that PCx has two different structures: α_4 and the αβ. The first consist of four identical subunits, with about 120 kDa each, and it is found in most organisms ranging from bacteria to vertebrates. These enzymes structure has three functional domains identified: carboxylase domain; the biotin carboxylase carrier domain and carboxyltransferase. [51, 54] The αβ form has two subunits, with an approximately 70kDa polypeptide carrying the biotin (α) and the non-biotinylated polypeptide with 55 kDa (β) [55]. There are some sequence similarities within the biotin-dependent carboxylases, which is not surprising since they share common reaction mechanisms [51].

Figure 2.8 – Protein structure of pyruvate carboxylase. Red and green area relates to carbamoyl phosphate synthetase. Blue area is the biotin carboxylase carrier domain. Yellow area is HGML-like domain. Purple area conserved carboxylase domain. Orange area biotin attachment domain [56].

Above it is represented the primary structure prediction for PCx in *S. coelicolor* A3 (2), according with PFam prediction (Figure 2.8). Additionally, the domains constituting the protein were identified by comparing nucleotides and amino acid sequence [56]. The first two domains, highlighted in green and red are similar to a carbamoyl phosphate synthase which is usually responsible for the ATP-dependent synthesis of carbamoyl phosphate from bicarbonate. The orange domain is a biotin attachment domain which has a conserved lysine residue involved in biotin binding. The yellow region is a conserved HMGL-Like (Hydroxymethyl Glutaryl-Coa Lyase) region identifying this protein as an HMGL-Like family member. This domain is a characteristic region of various aldolase enzymes identifying it as a protein of this family [57]. Finally the blue domain represents a biotin carboxylase carrier conserved region in pyruvate carboxylases. This domain is found adjacent to the HMGL-like domain and often close to the biotin attachment domain of biotin requiring enzymes.

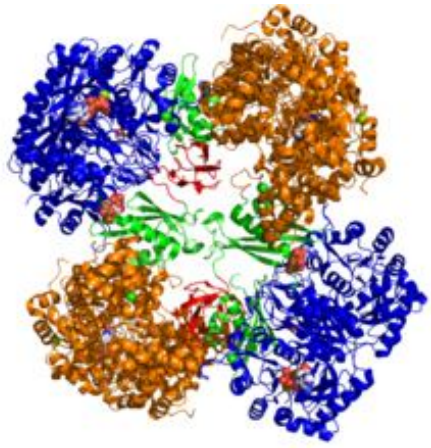

Figure 2.9 – Three dimensional prediction of an α_4 Pyruvate carboxylase from *Rhizobium etli*. Blue – Biotin carboxylase domain; Green – Allosteric linking domain; Red – Biotin binding domain; Orange – Carboxyl transferase domain[56]

On Figure 2.9 it is relevant to note the arrangement of the quaternary structure forming a tetrahedral geometry facilitating the movement of biotin carrier domain between neighbouring active site pairs [58].

As many other enzymes PCx is subjected to allosteric regulation by different molecules, although this can turn out to be quite complicated since the two structural forms seem to have different mechanisms of regulation. L-aspartate and 2- oxoglutarate non- competitively inhibit

the activity of the enzyme while AMP, ADP and pyruvate inhibit PCx in a competitive manner. [59-61] On the other hand, acetyl-CoA, enhances the activity of PCx with a special focus on carboxylation of biotin step. Although it was not a significant improvement, it was proved that acetyl-CoA had a positive influence on PCx activity. Strikingly, the αβ structure was found to be completely independent activity from acetyl-CoA [52, 55, 60, 62]. Regulation of PCx by these three molecules is likely to have a physiological role in maintaining an equilibrium between catabolic and anabolic reactions because oxaloacetate is a precursor of molecules like aspartate and is directly related to acetyl-CoA by the reaction oxaloacetate to citrate in Krebs cycle [59]. It was also reported that PCx expression also affects proteome since it was proved that its presence is important to alcohol oxidase and the deletion of PCx gene causes the accumulation of inactive alcohol oxidase in the methyltrophic yeast, *Hansenula polymorpha*. [63].

3. Materials and Methods

3.1. Chemicals and Consumables

The chemical and biological reagents and equipments used through this project were obtained from. Fisher Scientific, NEB, Promega, SIGMA, BioLine and Invitrogen

3.2. Bacterial Strains

3.2.1. *Streptomyces coelicolor* A3 (2)

Introduced by Hopwood, in 1957[64], this organism is used as a system model to study the Streptomyces genus the strain M145 is a prototrophic derivative of *Streptomyes coelicolor* A3(2).

3.2.2. Escherichia coli

Throughout this project three different strains of *E. coli* were used .

Table 3.1 - Escherichia coli strains used in this project

DH5α	Storage strain used as host for plasmid DNA
ET-12567-pUZ8002	Strain used to conjugate plasmids into *S. coelicolor* A3(2) – Chemical or electrocompetent cells
BL-21	Strain used to overexpress the proteins

3.3. Transposons, Cosmids and Plasmids

In Table 3.2 are described the plasmids, cosmids and transposons used in this project

Table 3.2 – Transposons, Cosmids and Plasmids used in this project

Vector	Description	Resistance Marker	References
SuperCos-1	Backbone for cosmid library Insertional Mutagenesis - Gene knockout	Kan^R;Amp^R	[65]
Tn5602	Transposon element with Apramycin resistance marker	Apr^R	[66]
SC_JC_01_pyc::Tn5062	Super Cosmid1 ligated to Tn5062 – Gene knockout	Apr^R;Kan^R;Amp^R	This work
pGEM-T Easy Vector	Gene Complementation	Amp^R	(Promega)
pIJ6902	Gene Complementation	Apr^R;Tst^R	[67]
pET100-DTOPO	Protein overexpression	Amp^R	(Invitrogen)
pJC_01_pyc	pGEM-T ligated to SCO0546 – Gene Complementation	Amp^R	This work
pJC_02_pyc	pIJ6902 ligated to SCO0546 – Gene Complementation	Apr^R;Tst^R	This work
pJC_03_pyc	pET100-DTOPO ligated to SCO0546 – Protein overexpression	Amp^R	This work

3.4. Oligonucleotides

To isolate the gene SCO0546 some oligonucleotides were required which can be consulted in Table 3.3.

Table 3. 3 – Oligonucleotides used in this project

Primer name	Sequence (5' to 3')	Melting Temperature (ºC)
SCO0546pycF	CACCATGTTCCGCAAGGTGCTG	73.8
SCO0546pycR	TCAGGCGATTGGACGAGAAGATC	71.6
SCO0546pycCompF	AGGCTGAAGGGATCAAGAATGT	61.3
SCO0546pycCompR	GTCGAGCACTTCAACAAGTACG	60.0

3.5. Media and Solution Preparation

Every solution was prepared using the recipes described above, using deionised water as solvent. When appropriate, the solutions were autoclaved for 20 minutes at 121ºC.

Table 3. 4 - Solutions used in this work

Solutions	Reference/ Composition
Medium	
Lysogeny Broth	Bertani, 1951 [68]
Minimal Media	Hopwood et al, 1967[69]
Mannitol Soya-Flour	Hobbs et al 1989 [70]
R2	[71]
R2YE	[71]
R5	[71]
Supplemented Liquid Minimal Media	Strauch et al., 1991[72]
YEME	[71]
2xYT	[71]
Other Solutions	
Resuspension Solution (pH 8)	Glucose 50 mM Tris HCl 25 mM EDTA 10 mM
Lysis Solution (250 mL)	NaOH 0,2 N SDS 1%
Neutralization Solution (100 mL)	Potassium Acetate (60 mL) 5M Acetic Acid (11.5 mL)

Table 3. 5 – Solutions used in this work (continued)		
Solutions	**Reference/ Composition**	
	Other Solutions	
Fixative (20 mL)	Gluteraldehyde	35 µL
	Formaldehyde	1.4 mL
PBS (pH 7.4; 1000mL)	NaCl	8 g/L
	KCl	0.2 g/L
	Na_2HPO_4	1.44 g/L
	KH_2PO_4	0.24 g/L
Buffer A	Tris HCl (pH 7)	50 mM
	Glycerol	10%
	Imidazole	20mM
Buffer B	Tris HCl (pH 7)	50 mM
	Glycerol	10%
	Imidazole	500mM
Master Mix (600 µL)	Tris HCL (pH 7)	1 mM
	ATP	0.02 mM
	$MgCl_2$	0.05 mM
	KCl	0.10 mM
	$NaHCO_3$	0.15 mM
	NNADH	0.15mM

3.6. Methods for modifications in bacteria

3.6.1. Preparation of chemically competent cells

From an overnight culture incubated at 37ºC, shaking at 220 rpm, a dilution of 1:100 was made into a 250 ml Erlenmeyer flask and incubated as mentioned above until an OD_{600} between 0.3 and 0.6 was reached, for the ET12567-pUZ8002 strain chloramphenicol (CHL) (25µg/mL) and kanamycin (KAN) (50µg/mL) were used as selective markers. The culture was centrifuged at 4,000 rpm for 7 minutes. The supernatant was discarded and the pellet was resuspended in 12.5 mL of an ice cold $MgCl_2$ solution (100mM) taking up to 5 min in this procedure. The solution was centrifuged once more at 4,000 rpm for 7 minutes. The pellet was resuspended in 3 mL of ice cold $CaCl_2$ (100mM) and then 22 mL of the same solution were added. The suspension was incubated on ice for 20 minutes and centrifuged for 10 minutes at 4,000 rpm. The pellet was resuspended in 1 mL of ice cold $CaCl_2$ (100mM) and 10% Glycerol. They were aliquoted in 100 µL and were stored at -80ºC.

3.6.2. Transformation in *E. coli*

3.6.2.1. Chemical Transformation

From the previously prepared chemically competent cells, 50 µL of this suspension was mixed with 2 µL of the appropriate plasmid or cosmid DNA and incubated on ice for 30 minutes.

The cells were heat shocked at 42ºC for 30 to 90 seconds and placed on ice again for 2 minutes. Immediately after this procedure, 1 mL of LB medium was added and cells were incubated ate 37ºC for 60 to 90 minutes. The cells were then spread with the appropriate antibiotics and left to incubate overnight at 37ºC.

3.6.2.2. Electroporation

Similarly to a chemical transformation, 2 µL of DNA are mixed with 50 µL of electro competent cells and incubated on ice for 30 minutes. The new volume is inserted in an electroporation cuvette and electroporated in a BioRad electroporator set at 10kV/cm. The cell suspension is used to inoculate 1 mL of 2xYT medium and it is incubated at 37ºC for 60 to 90 minutes. Finally the cells are spread on LB agar medium with the selective markers and incubated overnight at 37ºC.The electrocompetent cells were kindly provided by J. Hiltner

3.6.3. Plasmid or Cosmid DNA Isolation – Alkaline-Lysis Method

A single picked colony was grown on LB medium (5mL) with the appropriate antibiotics overnight. Two to three millilitres of the suspension were then harvested by centrifugation at 13000 rpm for 2 minutes. The supernatant was discarded and the pellet was resuspended in 100 µl of ice cold Resuspension Solution. 200 µL of Lysis Solution were added and the contents in the micro centrifuge tube were mixed by inverting. Then 150 µL of ice cold Neutralization Solution were added and the final mixture was vortexed until completely mixed. The suspension was centrifuged for 5 minutes at 13000 rpm and the supernatant was retrieved for a new eppendorf tube with 2 volumes of ethanol. The contents were mixed by inversion and incubated at room temperature for 2 minutes and then centrifuged for 5 minutes at 13000 rpm once more. The supernatant was discarded and the pellet was rinsed with ethanol (70%). The pellet was left to dry at room temperature. The dried pellet was resuspended in 50 µL of sterile water.

3.6.4 Spores stock preparation

From a previous vortexed spore stock, 100 µL were taken and spread on two MS plates for confluent growth. At the fifth day of incubation at 30ºC eight to ten mL of 20% glycerol were added to the plates and the spores were released by streaking the plates with a cotton bud. The suspension was withdrawn from the plates using a pipette and aliquoted in 1mL cryo tubes and stored at -20ºC.

3.6.5 Intergenic conjugation of plasmids and cosmids from *E. coli* to *Streptomyces coelicolor*

From an overnight culture of *E. coli* ET12567/pUZ8002 containing the desired plasmid or cosmid, a dilution of 1:100 was made and the culture was grown to an OD_{600} between 0.4 and 0.6. The cells were harvested by centrifugation at 10,000 rpm for 5 minutes and pellet was resuspended in 1mL of LB medium. This washing step was repeated once more. A spore suspension of *Streptomyces* was centrifuged for 5 minutes at 10,000 rpm and resuspended in 2xYT medium. The suspension was heat shocked at 50ºC for 10 minutes and left to cool. An aliquot of this suspension (500 µl) was mixed with the same volume of the *E. coli* suspension and spread onto MS agar and incubated at 30º overnight. On the next day the plates were overlaid with nalidixic acid (NAL-25µg/mL) and the relevant antibiotics. The plates were then incubated for two more days at 30ºC and then were patched for double crossovers screening on fresh NA agar with the relevant antibiotics.

3.7. Molecular Biology techniques

3.7.1. Polymerase Chain Reactions Experiments

The primers used in such experiments were designed accordingly to the need of their purposes, as it can be verified in chapter **4. Results**, and were ordered from SIGMA-ALDRICH. For more details consult **3.4. Oligonucleotides.**

Throughout this project PCRs were necessary twice, one first time to amplify the SCO0546 fragment containing natural promoters in order to perform the complementation and one second time to amplify the fragment in order to overexpress the protein associated with such gene, pyruvate carboxylase.

The Table 3.6 has the conditions used for the amplification of the gene regarding the complementation procedure while table 3.7 has the conditions used for the overexpression.

Table 3. 6 – Reaction conditions for the amplification of the gene SCO0546 – Complementation

Solution		**Thermo cycling conditions**		
Component	Volume (µL)	Steps	Temp. (ºC)	Time (min)
Sterile H_2O	36	**Initialization**	95	10
MyTaq buffer	10	**Denaturation**	95	1
Primer0546compF	1	**Annealing**	54	0.75
Primer0546compR	1	**Elongation**	72	1
Genomic M145 DNA	1	**Final elongation**	72	10
MyTaq Polymerase	1	**Holding Temperature**	12	
Fragment Size (bp)	3.840	**Number of Cycles**	35	

Table 3. 7 – Reaction conditions for the amplification of the gene SCO0546 – Overexpression				
Solution		**Thermo cycling conditions**		
Component	Volume (µL)	Steps	Temp. (ºC)	Time (min)
Sterile H2O	36	**Initialization**	95	10
MyTaq buffer	10	**Denaturation**	95	1
Primer0546compF	1	**Annealing**	60	0.75
Primer0546compR	1	**Elongation**	72	1
Genomic M145 DNA	1	**Final elongation**	72	10
MyTaq P polymerase	1	**Holding Temperature**	12	
Fragment Size (bp)	3.375	**Number of Cycles**	35	

3.7.2. Ligations

In order to perform the complete study of this metabolic route some ligations were necessary. Table 3.8 describes all the relevant information regarding these procedures.

Table 3. 8 - Conditions used to achieve the desired clones				
pGEM-T Easy Vector				
ng Vector used	**Vector size (bp)**	**ng of Insert**	**Insert size (bp)**	**Molar Ratio[1] (insert:vector)**
50	3015	150	3840	3:1
pET100 D-TOPO Vector				
ng Vector used	**Vector size (bp)**	**ng of Insert**	**Insert size (bp)**	**Molar Ratio[1] (insert:vector)**
45	5764	25	3375	1:1

1- The formula to calculate the Molar Ratio can be consulted on Annex Chapter, Equation A1

3.7.3. Restriction Digestions

The digestions were performed using the recipe described on Table 3.9 and incubated at 37ºC for at least 120 minutes. After this first step, 1 µL of RNase (20 µg) was added and the solution was incubated for more 30 minutes. Finally a heat inactivation was performed by leaving the solution for 20 min at a 65ºC water bath.

Table 3. 9 – Recipe used for Restriction Digestions	
Components	**Volume (µL)**
Enzyme Buffer	2
BSA	2[a]
DNA template	10[b]
Restriction Enzyme	1
Sterile H_2O	Up to 20

a- BSA was not required by all the enzymes used.

b- In case of high concentrated plasmid solutions, this value could be lower

3.8. Phenotype characterization assays

3.8.1. Solid media characterization

Plates with agar minimal medium and the desired carbon source (20% w/w), were used to streak the strains in study and were left to incubate at 30ºC for 10 days. A picture was taken every 24 hours.

3.8.2. Small scale screening in liquid medium

For this assay, 15 µL of spores were washed from the glycerol stock and inoculated in 1.5mL of Supplemented Minimal medium. Three glass beads (2mm diameter) were added in every well. The plate was incubated at 30ºC for 7 days.

On the 7^{th} day, 350 µL of the supernatant were used to determine actinorhodin concentration (**3.8.2 Actinorhodin assay**) and the biomass was weighted (**3.8.3 Cell Dry Weight Determination**).

Although not all the wells were used for this assay, none was left empty filling the extra wells with 1.5 mL of SMM and three glass beads to prevent evaporation of the wells which contained cells.

3.8.3. Actinorhodin Assay

To determine the actinorhodin concentration, one volume of a NaOH solution (1N) was added to the solution being analysed and it was centrifuged for 5 minutes at 10,000 g. The supernatant was withdrawn to another tube and the absorbance was then checked at 633 nm using the solution of NaOH as a blank.

The molar extinction coefficient was 15.135 $M^{-1}cm^{-1}$ and the pathway length was 1 cm. The concentration could be calculated using the Lambert-Beer Law. (See Equation A2 in Annex Chapter)

3.8.4. Cell Dry Weight Determination

The biomass was withdrawn with a pipette and filtered on a vacuum filtration system using pre-weighted dried filter papers. To ensure that all the biomass was withdrawn, deionised H_20 may be added to each well in order to help retrieving all of the biomass which was also washed twice to remove remaining salts of the medium. The filter papers containing biomass were then dried on a microwave oven until the weight of the papers remains constant (10

minutes at 75%of maximum power). The biomass weight was estimated by calculating the difference between the papers before and after filtration step.

3.8.5. Pregermination of *Streptomyces* spores

20mL of 2xYT medium were inoculated with 20 µL of spore suspension in a 250mL Erlenmeyer flask containing a coiled spring, The flask was incubated at 30ºC and 220 rpm until it was possible to see spores starting to germinate under bright the bright field microscope, usually this procedure took from 6 up to 8 hours.

The culture was spinned at 1000 x g for 5 min, the supernatant was discarded and the biomass was resuspended in 5mL of the medium to be used in the following steps of the experiment.

The spore concentration was estimated by checking the absorbance at 450 nm (1 unit of OD_{450} = 4 x 10^7 spores per mL).

3.8.6. Growth curve

From a culture of pregerminated spores, a volume corresponding to 1x10^8 spores was withdrawn and incubated in 400mL of Supplemented Minimal Media (SMM) in a 2L Erlenmeyer flask containing a coil spring at 30º and 220 rpm for 30 hours. From this moment onwards, samples were taken to measure the biomass weight and actinorhodin concentration using the methods mentioned previously.

3.8.7. Microscopy Assay

3.8.7.1 Cultivation on cover slips

Cover slips were inserted with a 45º angle into Minimal Media agar plates. The area between the cover slips and the agar was inoculated with a spore suspension diluted 1:10. The plates were incubated at 30ºC and samples were taken after 3, 5 and 7 days of incubation.

3.8.7.2 Preparation of the slides

The cover slips were removed from the agar and their backside was cleaned with ethanol, the cover slips were placed over two toothpicks with the side containing bacteria upwards. To each cover slip 400 µL of fixative was added and left to incubate for 15 minutes at room temperature.

The cover slips were then washed twice with PBS, air dried and washed again with PBS. The excess solution was removed and the cover slips were mounted onto the slides.

The cover slips were ready for analysis under the microscope using bright field with 100x magnification.

3.8.8. Preparation of cell free extracts

After the incubation procedures cells were harvested by centrifugation (4000rpm for 10 minutes) and resuspended in the buffer of interest.

The suspension was then introduced in the French press and collected after being under a higher pressure environment (Cell Perss I.S.H.on High Ratio – 1000psi). This procedure was repeated three times.

The sample was then centrifuged once again (4,000 rpm for 10 minutes) and the supernatant was retrieved to a new tube. The extracts were used for protein purification or for the enzyme activity assay.

3.8.9. Enzymatic assay

To perform the enzymatic assay, 50 µL of the spore suspension were incubated in 50 mL of YEME medium in 250mL Erlenmeyer flasks, containing a spring coil, for 24 hours at 30ºC and 220 rpm. The cell extract was obtained using the method explained in **3.8.7. Preparation of cell free extracts** and using Tris HCl (50 mM; pH 7) as resuspension buffer.

All the solutions used for this assay and their volumes are described in Table 3.10.

Table 3. 10 – Solutions used in the enzymatic assay

Solutions	Volume (µL)
Master Mix	600
Cell Extract	100
Malate Dehydrogenase	2U[a]
Pyruvate	b
H_2O	Up to 1mL

a- In this case it was important to make sure that 2 enzyme units were introduced rather than a specific volume.

b- Pyruvate volume was variable throughout the assay.

The master mix composition can be verified on **3.5 Media and Solution preparation**. It is also important to highlight the order in which those solutions were added. The first element to be introduced in the glass cuvette was water followed by the cell extract and Malate dehydrogenase. Pyruvate and the Master Mix were added by last, at the same time.

In this experiment the concentration of NADH was being assayed by checking the absorbance at 340 nm for 3 minutes making a reading every thirty seconds. The molar

extinction coefficient was 6300 $M^{-1}cm^{-1}$ and the wavelength path was 1 cm. In this assay one unit of enzyme activity is defined as that amount which catalyses the synthesis of **1** µmol of oxaloacetate per minute. The blank sample was made with all the components except cell extract and NADH.

3.8.10. Protein Concentration Assay

To estimate the protein concentration a Bradford assay was used. [73] First a calibration curve was assembled by mixing water, Bradford reagent (Bio-Rad) and a known amount of protein (BSA, 1 mg/mL) as described on Table 3.11.

Table 3. 11 – Samples for a calibration curve in a Bradford assay

BSA stock (µL)	H_20 (µL)	Bradford (µL)
0	**800**	
5	**795**	
10	**790**	200
15	**785**	
20	**780**	

The samples were mixed by vortexing and left to incubate for 5 minutes at room temperature. The OD_{595} was measured and the values plotted, forming the standard curve.

Samples of 200 µL of Bradford Reagent, 5 to 20 µL of sample to be analysed, and water up to 1 mL had their OD_{595} measured and the concentration was interpolated from the standard curve.

3.9. Pyruvate Carboxylase Overexpression and Purification

From freshly transformed *E. coli* BL21 with the plasmid of interest, a single colony was picked and incubated overnight in 5mL of LB medium with the appropriate antibiotics (37ºC, 220 rpm). That same culture was then used to inoculate 500 mL of LB medium in a 1:10 dilution for 5 hours under the same conditions. From which 20 mL were used to inoculate 1 L of Lb medium that was incubated until it reached an OD_{600} between 0.4 and 0.6 (37ºC, 220 rpm).

At this moment IPTG was added to cell culture up to a final concentration of 1mM. The cells were then grown overnight at 15ºC and 220 rpm. Throughout this procedure two samples of 1 mL were withdrawn, one prior to the induction with IPTG and other after the overnight incubation at 15ºC.

3.9.1. SDS PAGE

The sample before induction was centrifuged for 1 minute at 10,000 g and 900 µL of the supernatant were discarded. To the remaining 100 µL of the suspension, 100 µL of SDS buffer were used to resuspend the cell pellet and the 200 µL were incubated in a water bath at 95ºC for 5 minutes. The sample was stored at -20ºC for further use.

The second sample was centrifuged under the same conditions but only 880 µL were discarded. 20 µL were transferred to a new eppendorf tube along with the same volume of SDS buffer and this new solution was cooked for 95ºC for five minutes, creating a sample of the supernatant to run on a SDS PAGE

To the remaining 100 µL it was given the same treatment as to the first sample. 100 µL of SDS buffer were added and used to resuspend the cell pellet, this suspension was then incubated for 5 minutes at 95ºC.

After such treatment all samples were used to run an SDS PAGE which was prepared according to the protocol mentioned on GE HealthCare Amersham ECL Gels protocol for 4-12% gradient gels.

3.9.2. Protein Purification

The rest of the cell culture from the over expression assay was centrifuged, the cell pellet was resuspended in 20 mL of Buffer A and a cell extract was obtained using the method explained in **3.8.7. Preparation of cell free extracts**.

The cell extract was centrifuged at 4,000g for 10 minutes in order to retrieve the supernatant and discard the cell pellet.

The cell free extract was loaded onto a HisTrap FF crude 1mL column from GE Healthcare and then using Akta Purifier to purify the protein as the pET100 D-TOPO vector adds an HisTag to the protein which is attracted to the nickel on the column. For the gradient elution it was used Buffer B.

3.10. Bioinformatic analysis

Phylogenetic and molecular evolutionary analyses were conducted using MEGA version 5.05[74] with conditions described on Table 3.12.

Table 3. 12 – Parameters used on the alignment exercise	
Statistical method	**Neighbour-joining**
Test of Phylogeny	Bootstrap method (1000 replications)
Substitution Model	Poisson Model
Alignment Method	Clustal W[75]
Gap Opening Penalty	10
Gap Extension Penalty	0.2
Protein Scoring Matrix	BLOSUM

The selected organisms were chosen bearing in mind the available information on Pyruvate Carboxylase and their relevance to this work and they are announced on Table 3.13.

Table 3. 13 – List of Selected organism for alignment exercises
***Streptomyces coelicolor* A3(2)**
Mycobacterium tuberculosis
Arthrobacter globiformis
Corynebacterium diphetriae
Sinorhizobium meliloti
Rhizobium etli
Bacillus subtilis
Mus musculus
Homo sapiens

4. Results

In this work the characterisation of the Phosphoenolpyruvate-Pyruvate-Oxaloacetate-node in *Streptomyces coelicolor* A3 (2) was carried out focusing in the biochemical characterization of PCx and its role in production of actinorhodin and undecylprodigiosin. The first part of the work involved the genetic manipulation of *S. coelicolor* A3 (2) genome to eliminating the SCO0546 gene, presumed to encoding pyruvate carboxylase (PCx).

4.1. Construction of M145Δpyc::Tn5062 mutant

Using the *Streptomyces* database available online (StrepDB [65]) it was possible to identify the SCO0546 gene which is predicted to encode PCx in *S. coelicolor.* Knocking out of SCO0546 was done by transposon mutagenesis using an available transposon insertion library at University of Swansea [66, 76]. Below it is depicted a schematic representation of the transposon used:

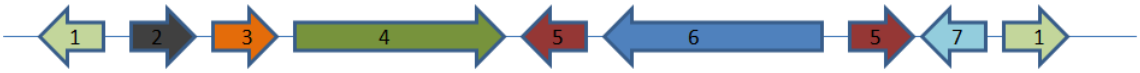

Figure 4.1- Transposon Tn5062. 1-Inverted Repeats, 2- Translational Stop Codon, 3- Streptomycetes Ribossome Binding Site, 4- EGFP, 5-T4 Terminators, 6-Aac(3) IV –Apramycin, 7-Origin of Transfer.

The transposon Tn5062 ligated into SuperCosmid1 was subjected to a restriction digest to confirm that it was correct. The enzymes used for this procedure were identified by doing a restriction digestion *in sillico* using Clone Manger 6® software. Two enzymes were identified which would be able to generate a set of DNA fragments that would allow the identification of the cosmid ligated to the transposon. If the cosmid is well ligated to the transposon then a restriction reaction with *Hind*III and *Xho*I should yield a set of fragments with the sizes described on Table 4.1.

Table 4. 1 – Fragments resulting from SC_JC_pyc::Tn5062 digestion	
Fragments size (bp)	**Enzymes Used**
21922	HindIII XhoI
10877	
7687	
1022	
841	
699	
694	

After digestion, a gel electrophoresis was done and the result obtained is shown in Figure 4.2.

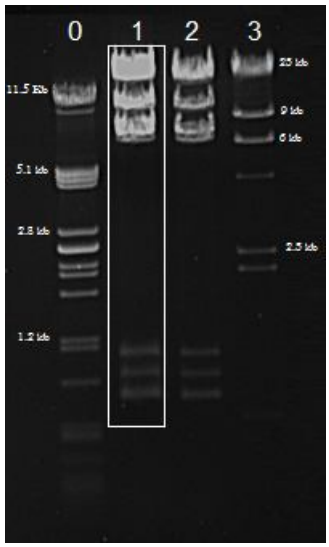

Figure 4.2 – Gel electrophoresis from F11.2.G07 digestion with HindIII and XhoI. 1 – λPst Ladder; 2 – Cosmid Digestion, sample 1; 3 – Cosmid Digestion, sample 2; 4 – λHindIII Ladder

The comparison of the predicted fragments with obtained band pattern confirms that clone SC_JC_01 contains the transposon well inserted in the cosmid. After this confirmation we proceeded to the conjugation process to transform *S. coelicolor* with this cosmid. This procedure was only possible because the *E.coli* strain used (ET12567-puZ8002) does not methylate DNA, a feature that is also observed in *S. coelicolor* A3(2) DNA [77]. Once the cosmid was confirmed, it was inserted into *E. coli* ET12567-puZ8002 and then transferred to *S. coelicolor* A3 (2) M145 by conjugation. After the conjugation the candidates obtained were screened to search for double crossover strains, which are presumed to have the PCx gene replaced by the transposon. These double crossover strains were identified and subsequently streaked for confluent growth and spores were collected and stored. Screening for double crossovers was made selecting the colonies surviving on apramycin and not on kanamycin

since apramycin is the selective marker of the transposon Tn5062 and kanamycin is the selective marker of the cosmid. Therefore, selecting a colony surviving only on Apramycin, means that it has kept the transposon but has lost the cosmid implying a permanent double crossover event of the transposable element into the hosts DNA creating the mutant M145Δpyc::Tn5062.

4.2. Phenotypic analysis of the M145Δpyc::Tn5062 mutant

Phenotypic characterisation of S. coelicolor M145Δpyc::Tn5062 mutant was carried out both in liquid and solid media. For the experiments carried out in solid media the mutants were grown on minimal media with a set of seven different carbon sources (acetate, citrate, pyruvate, N-Acetylglucosamine, tween 80, glucose) and in four types of rich medium (MS, R21 R5 R2YE). The strains were incubated for ten days and everyday a picture was taken. Within the ten days that comprise this experiment the pictures of the seventh day were considered the most representative and are the ones shown in Figure 4.3. Production of Act and Red was also assessed based on the blue or red pigmentation of the colonies.

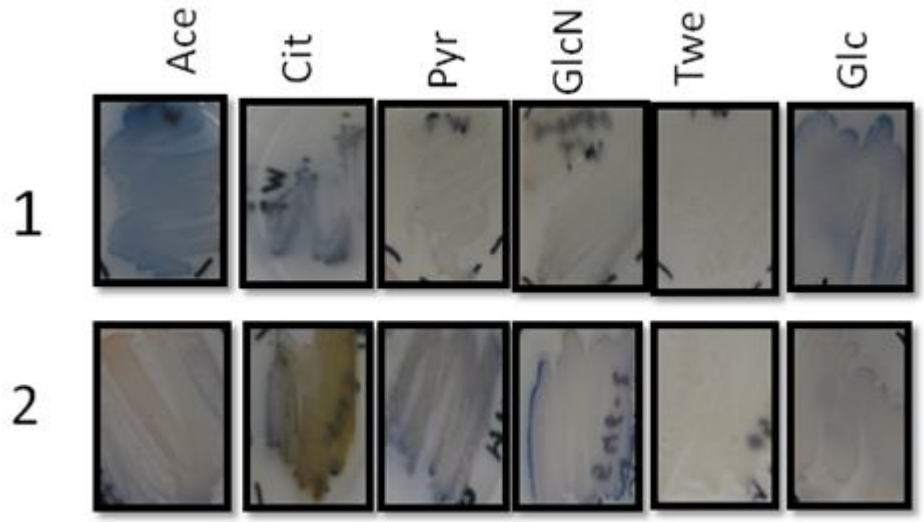

Figure 4.3 - Phenotypical differences between Wild type M145 (1) and mutant M145Δpyc::Tn5062 (2) on Minimal Media with different carbon sources. From Left to right: Acetate (Ace), Citrate (Cit), Pyruvate (Pry),N-Acetyl Glucosamine (GlcNAc), Tween80 (Twe) and Glucose (Glc).

The results obtained show a clear difference between the growth of the two strains in almost every type of carbon source, with the exception of Tween 80. When acetate is used as the sole carbon source, the production of Act is higher in the wild type than in the mutant, which in turn exhibits a higher production of Red. The same result is observed when citrate is used as a carbon source. When pyruvate is used as a carbon source, the production of Act is only

observed in the mutant strain. When GlcNAc is used as a carbon source the results obtained are similar to those obtained with pyruvate, although the production of the antibiotic is slighter than the one observed for pyruvate. When Tween 80 was used as a carbon source no significant difference in growth of the two strains was observed. Wild type cells exhibited a higher production of Act when grown in MM with glucose, compared to the mutant strain.

The results obtained on the four types of rich media used are shown on Figure 4.4.

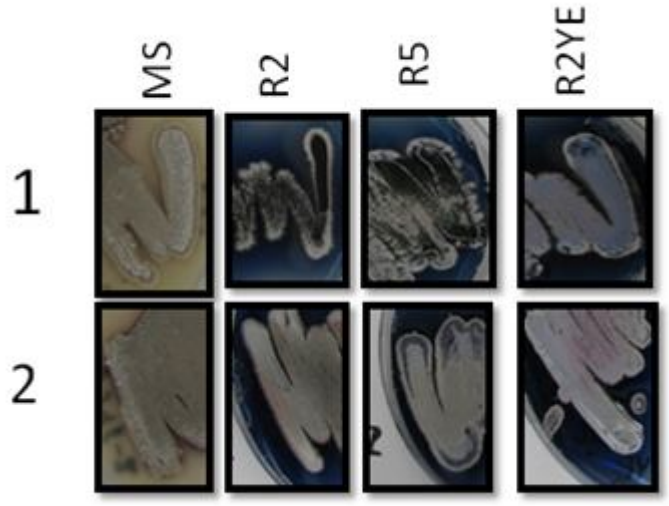

Figure 4.4 – Phenotypical differences between wild type M145 (1) and mutant M145Δpyc::Tn5062 (2) on four types of Rich Media

In this case there is almost no difference in growth of the two strains, although the growth rate of the mutant was found to be slightly below the one of wild type cells. In MS medium no differences in antibiotic production was observed between mutant and wild type cells. In R2 and R5 a higher concentration of Act is observed in wild-type cells, when compared with the mutant, which evidenced by the dark blue colour present even within the mycelium. In R2YE medium production of Act was also higher in wild-type cells while the mutant still seems to be producing Red.

A phenotypic analysis of M145Δpyc::Tn5062 growth and of wild type cells in liquid media was also carried out in this work. In this case the mutant and wild-type strains were cultivated in 24-wells plates containing the different media tested. On the seventh day, the picture shown on Figure 4.5 was taken.

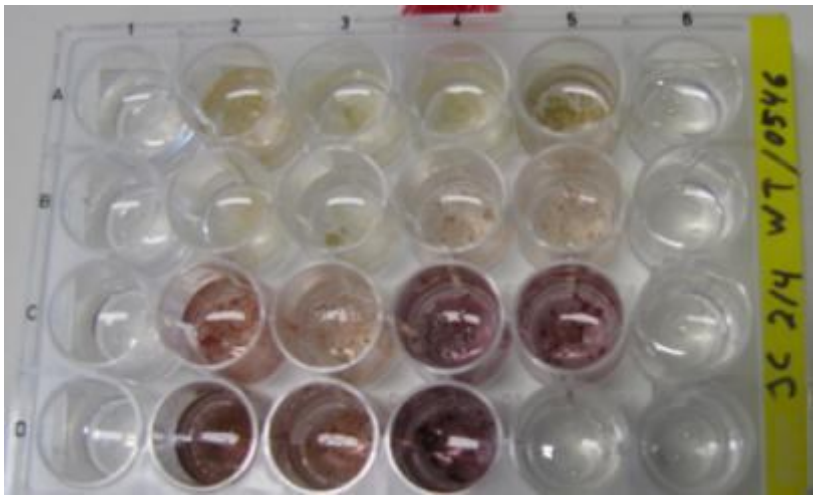

Figure 4.5-Picture obtained from the 24-well plate assay at the 7th day of incubation. A2-B2 – Wild type; B3-C3- M145Δpyc::Tn5062from spores aliquot 1; C4-D4- M145Δpyc::Tn5062 from spores aliquot 2

The biomass and concentration of actinorhodin at the end of the incubation period are shown on Figure 4.5. In this case each 5 wells were measured and an average was calculated. The first 5 wells (positions A2-B2) correspond to wild type wild-type cells in which it can be seen that there is almost no actinorhodin produced evidenced by the lack of colour in the wells. The next five wells correspond to one aliquot of spores of the mutant strain and it can be seen a slight change in the colour indicating the presence of some antibiotic. The last five wells (C3-D4) are from a different aliquot of mutant spores in which it can be seen an intense coloration which is indicative of a higher antibiotic production.

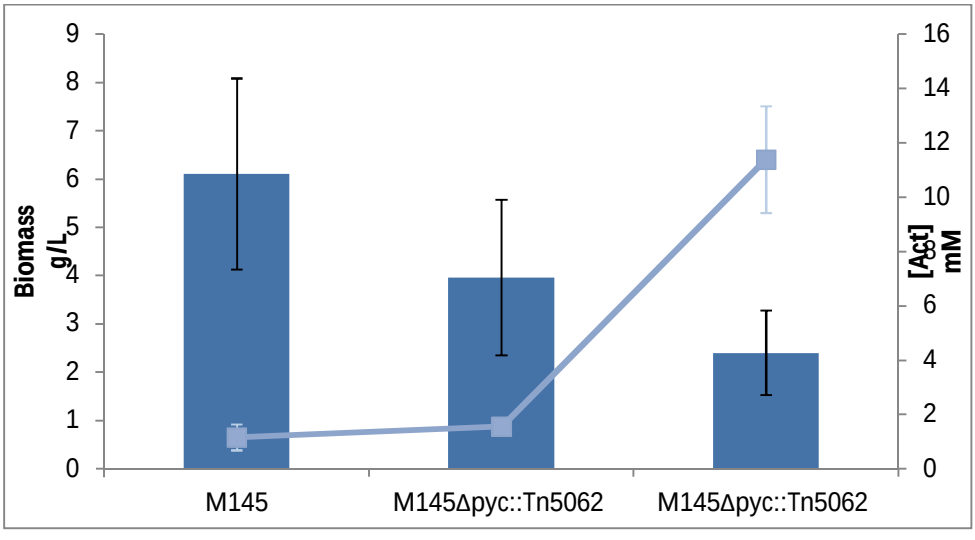

Figure 4.6 – Data recovered from 24 Wells-plate assay. Dark Blue bars – Biomass (g/L); Light Blue line – actinorhodin concentration (mM)

Biomass produced by the two aliquots of mutant's spores reached 3.96g/l and 2.4g/l while wild type cells achieved 6.1 g/L. However, antibiotic production has in inversed pattern

since mutant cells produced higher amounts of Act than wild-type cells, 1.54 mM and 11.4 mM compared to 1.15 mM.

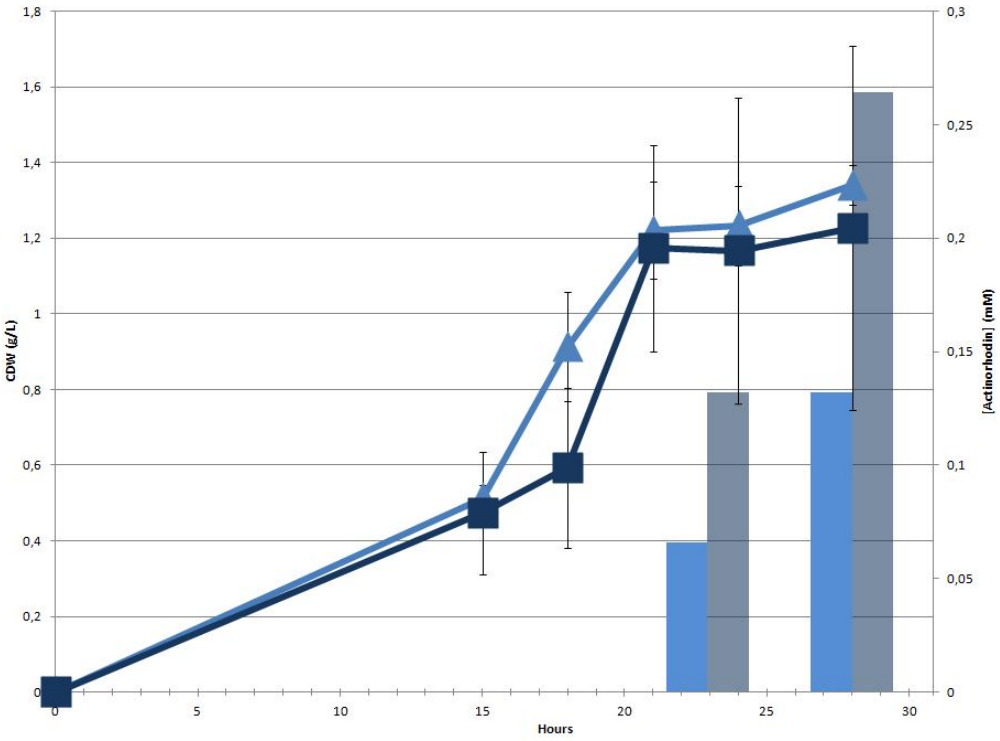

Figure 4.7 –Measurements on CDW and actinorhodin concentration during a Growth curve performed on Supplemented Minimal media with Glucose as carbon source.

The last assay performed in liquid media was a growth curve. The mutant and wild type were incubated for 28 hours and several samples were collected throughout this time resulting on the plot described on Figure 4.7. The results obtained in this assay show that after 22 hours of growth biomass of wild type culture reached a final titer of 1.34 g/L while the mutant culture only achieved 1.22g/L. The growth rate of the two populations was also slightly different: 0.61g/Lh for wild-type cells and 0.55 g/Lh for the M145Δpyc mutant. During this time the deletion mutant produced a higher titer of actinorhodin than wild-type cells, 0.26 mM of compared to 0.13 mM (Figure 4.7).

As the microorganism being studied has a distinct life cycle, this phenotypic trait was also analysed in order to analyse if PCx expression had any influence on the spore formation. The pictures resulting from the microscopy analysis are described in the following image 4.8. The pictures correspond to the third, fifth and seventh day of incubation.

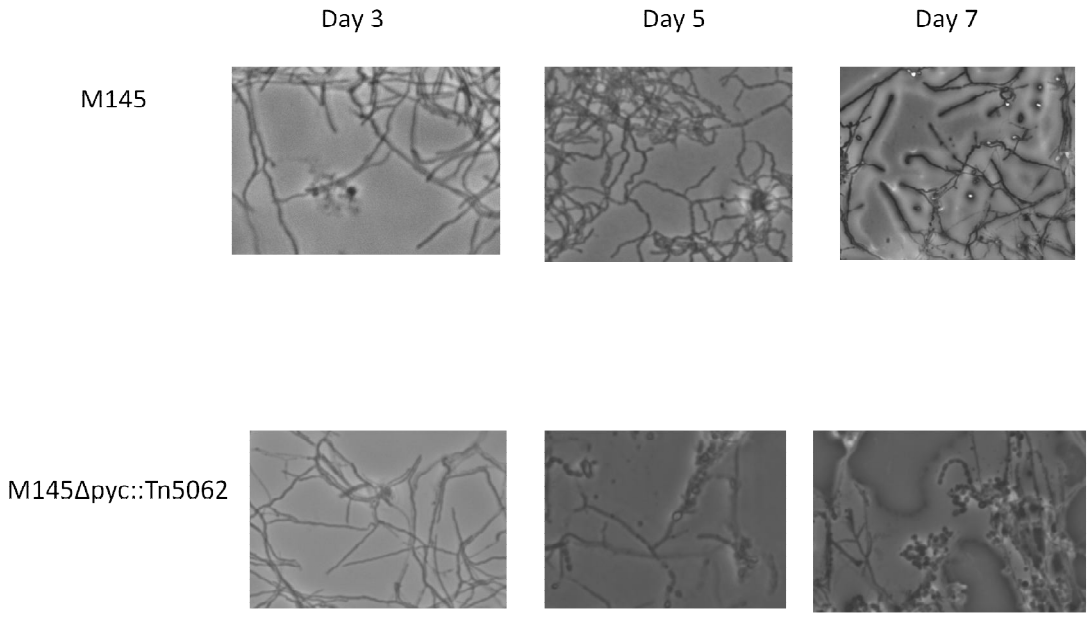

Figure 4.8- Pictures taken through microscopy, to wild type and the mutant, on day 3,5 and 7 of incubation.

The results obtained from microscopy showed no differences between growth of the strains indicating that PCx does not take part in the differentiation of *S. coelicolor* A3 (2) life cycle stages. Consistently, proteins of central metabolism have not yet been directly implicated in the organisms development [78].

4.3. Complementation

To see if the phenotypes attributed to the M145Δpyc mutant are indeed attributable to the elimination of SCO0546 gene, a complementation strategy was designed aiming to reclone the gene in a plasmid and transforming it into *S. coelicolor*. This part of the work has started with the optimisation of the amplification of the gene by PCR which was found to be maximal under the experimental conditions described in chapter **3.7.1. Polymerase Chain Reactions Experiments.** In Figure 4.9 it is depicted the result of an amplification experiment of SCO0546.

Figure 4.9-Gel electrophoresis of PCR amplification for complementation of M145Δpyc::Tn5062. 0-1Kbp Promega marker; 1-PCR Product

The amplified fragment should have 3,840 bp which is in agreement with the results obtained in image 4.9 where it is possible to see a band between 3 kbp and 4kbp. The amplified fragment is slightly bigger than the gene size (3,375 bp) in order to include some flanking sites that may contain a natural promoter. The amplified fragment was ligated into pGEM-T vector [79] yielding plasmid pJC_01_pyc::Tn5062 (Figure 4.10). The polymerase used adds an adenosine nucleotide to the 3´end which is complementary to the Thymidine ends of pGEM-T easy vector.

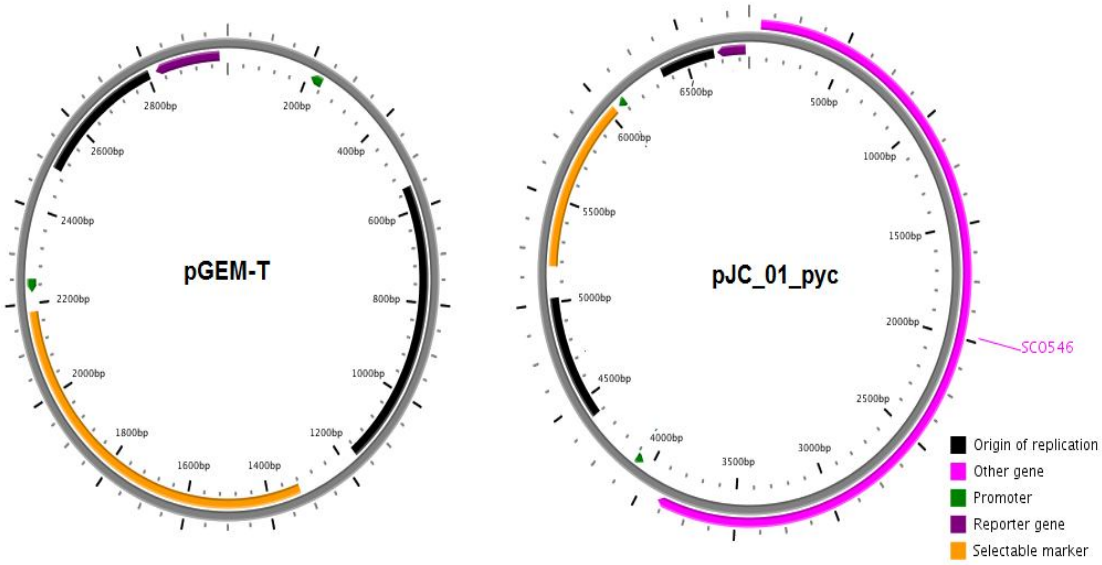

Figure 4 10- Vector map for Plasmid pGEM-T and pJC_01_pyc

The pGEM®-T Easy Vector contains the coding sequence of β-galactosidase interrupted by the cloning site enabling the identification by colour screening of the colonies obtained. Colonies containing the PCR product inserted in the vector produce white colonies as they are not able to hydrolyse the X-gal present in the media. Therefore blue colonies indicate an active β-galactosidase and consequently empty vectors. The white colonies obtained had their plasmid DNA extracted to verify the insertion of the fragment. For this, plasmid DNA was digested with *Eco*RI enzyme which is predicted to result in the fragment pattern described in Table 4.2.

Table 4. 2 – Fragments resulting from pJC_01_pyc digestion

Fragments size (bp)	Enzymes Used
3858 2997	*Eco*RI

The plasmid was isolated from *E. coli* DH5α, digested and confirmed in an electrophoresis gel (Figure 4.11)

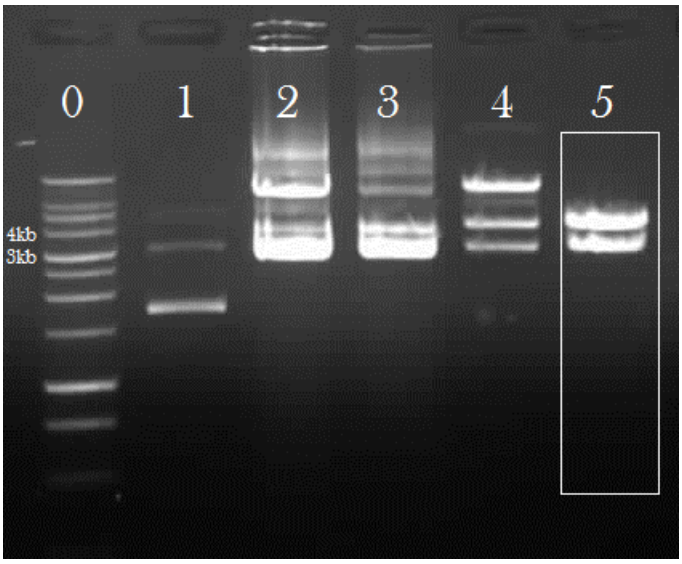

Figure 4. 11 – Gel electrophoresis of pGEM-T digestion with EcoRI. 0 – 1 kb Promega ladder; 1-5 pJC_01_pyc::Tn5062 digestion with EcoRI.

The subsequent steps of the cloning strategy implied removal of the fragment cloned in pJC_01 through digestion with EcoRI and subsequent insertion into the pIJ6902 plasmid, an Integrative P_{ita} expression vector that allows expression of the PCx gene in S. coelicolor. Before this, the pJC_01 plasmid was digested with EcoRI and the fragment presumed to contain the gene (having around 3858 bp) was excised from the gel and sent to sequencing using T7 and SP6 as primer sites (Table 4.3).

Table 4. 3 – Alignment score of pJC_01_pyc with M145 Genome	
T7 RNA polymerase promoter	
Score	1965 bits (991)
Identities	1036/1046 (99%)
Gaps	5/1046 (0%)
SP6 RNA polymerase promoter	
Score	1913 bits (965)
Identities	1035/1048 (98%)
Gaps	9/1048 (0%)

The information on Table 4.3 confirms that the fragment contains the PCx gene and can be used for the subsequent cloning steps. Plasmid pIJ6902 has an *Eco*RI site between a transcription terminator of a phage fd and a thiostrepton inducible *tip*A promoter which will be used to perform the cloning steps.[67]. A schematic representation of how the pJC_02_pyc plasmid would look like after cloning of the PCx fragment in the pIJ6902 plasmid is shown in Figure 4.12.

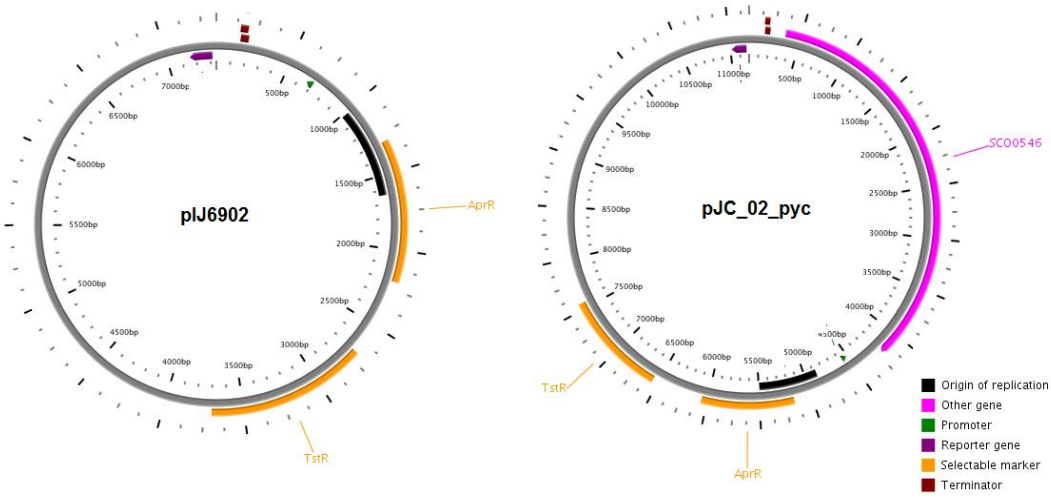

Figure 4.12 – Vector map for Plasmid pIJ6902 and pJC_02_pyc with the two possible insert orientations.

From the *in sillico* analysis it was found that a digestion with *Kpn*I would be suitable to identify the correct clone resulting in the fragments described on Table 4.3.

Table 4. 4 - Fragments resulting from pJC_02_pyc digestion

Fragments size (bp)		Enzymes Used
A	B	
7579	8474	KpnI
2461	2461	
1158	263	

Although several ratios of insert:vector were tried in different ligation experiments it was never possible to get a clone with the expected restriction profile.

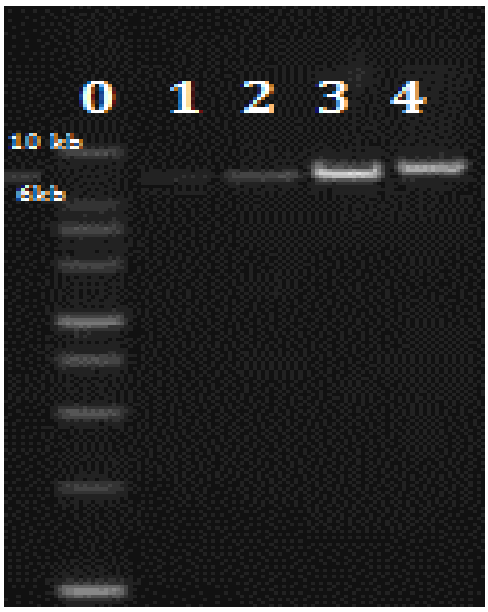

Figure 4. 13 – Gel electrophoresis of pIJ6902 digestion with KpnI. 0 – 1 kb Promega ladder; 1-4 – Samples digested with KpnI.

As it can be seen on Figure 4.13 there is only one band which does not correspond to the expected pattern described on Table 4.3 but to a digestion of an empty pIJ6902. To guarantee a proper ligation it is important to ensure a clean digestion product. In this case pJC_01 was digested with *Eco*RI which resulted in two products relatively close to each other. This proximity might have been problematic to separate the bands by cutting the gel, therefore it would be interesting to use a different approach on the digestion step and make a double digestion with another enzyme capable of breaking down the disposable fragment.

Utilising *Eco*RI combined with *Xmn*I would result in the fragment pattern described on Table 4.5 which could facilitate the extraction of the desired band.

Table 4. 5 – Fragments resulting from pJC-02 digestion

Fragments size (bp)	Enzymes Used
3858	EcoRI
1932	XmnI
1058	

Increasing the digestion time could also be important to achieve the construction of pJC_02.

4.4. Biochemical Characterisation of *S. coelicolor* pyruvate carboxylase

Biochemical characterisation of *S. coelicolor* PCx enzyme was also carried out in this work. For this, a bioinformatic analysis of S. coelicolor PCx was carried out to see the similarities and differences found the enzymes already described in other organisms ranging from bacteria to mammals. To confirm the structural prediction of PFam (already shown in Fig.2.8), a bioinformatic analysis was done focusing the key domains of the protein. Using annotated sequences from UniProt it was possible to align PCx from *S. Coelicolor* A3(2) with the same enzyme from other organisms. Some of the alignments in the more relevant regions of the proteins are described in Figure 4.14 to 4.17 (the carbamoyl phosphate synthase, HMGL-Like region and Biotin carboxyl carrier domains).

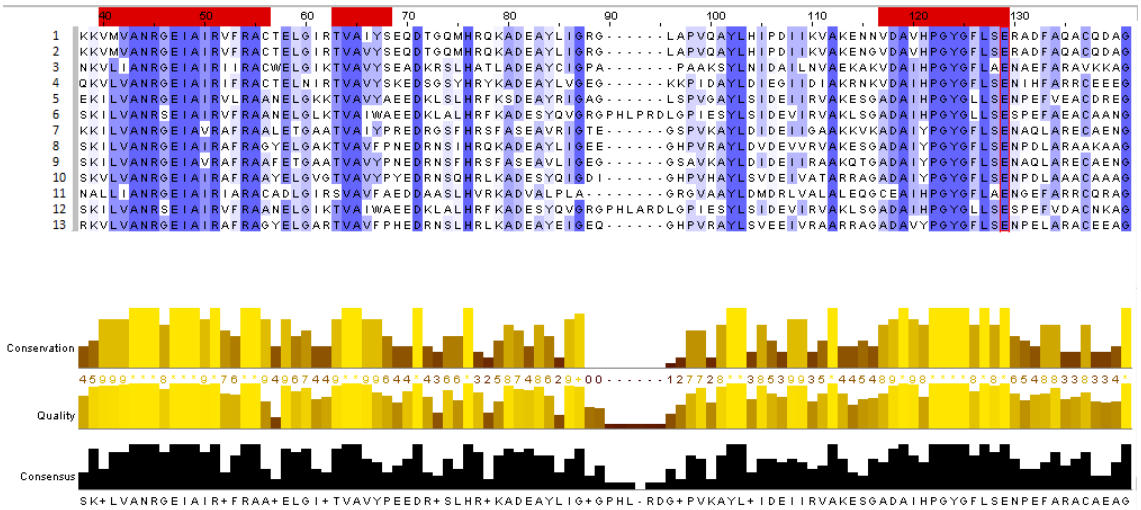

Figure 4. 14 - ClustalW alignment result on Carbamoyl phosphatase region. 1-*Homo sapiens;2-Mus musculus;3-Methanocaldococcus jannashii;4-Bacillus Subtilis;5-Rhodobacter capsulatus;6-Sinorhizobium meliloti;7-Corynebacterium glutamicum;8-Asthrobacter globiformis;9-Corynebacterium diphtheria;10-Pseudomonas aeruginnosa;11-Mycobacterium tuberculosis;12-Rhizobium etli;13-Streptomyces coelicolor*

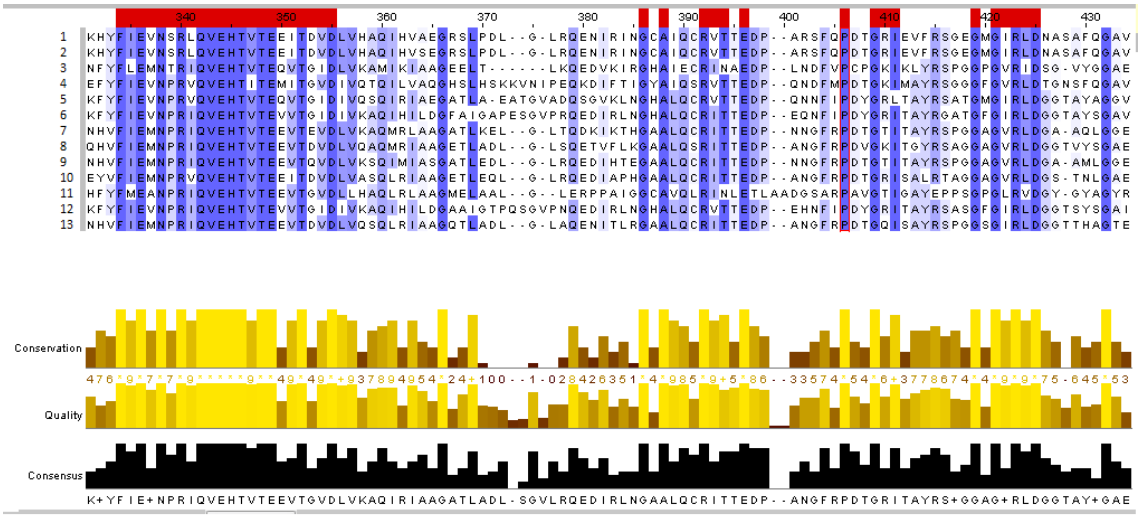

Figure 4. 15 – ClustalW alignment result on Biotin Carboxyl carrier region. 1-*Homo sapiens;2-Mus musculus;3-Methanocaldococcus jannashii;4-Bacillus Subtilis;5-Rhodobacter capsulatus;6-Sinorhizobium meliloti;7-Corynebacterium glutamicum;8-Asthrobacter globiformis;9-Corynebacterium diphtheria;10-Pseudomonas aeruginnosa;11-Mycobacterium tuberculosis;12-Rhizobium etli;13-Streptomyces coelicolor*

From the alignment pictures, namely 4.14 and 4.15, it is possible to see some conserved regions in the characteristic domains of these enzymes. These results strongly suggest that these proteins are likely to have an identical function in the metabolism and require ATP and biotin to perform the reaction. An alignment on the carboxylase domain shows also similarities between the sequence of PCx *S. coelicolor* with the sequences describe for other PCxs

suggesting that the mechanism involved for the carboxylation of pyruvate should be similar (Figure 4.16).

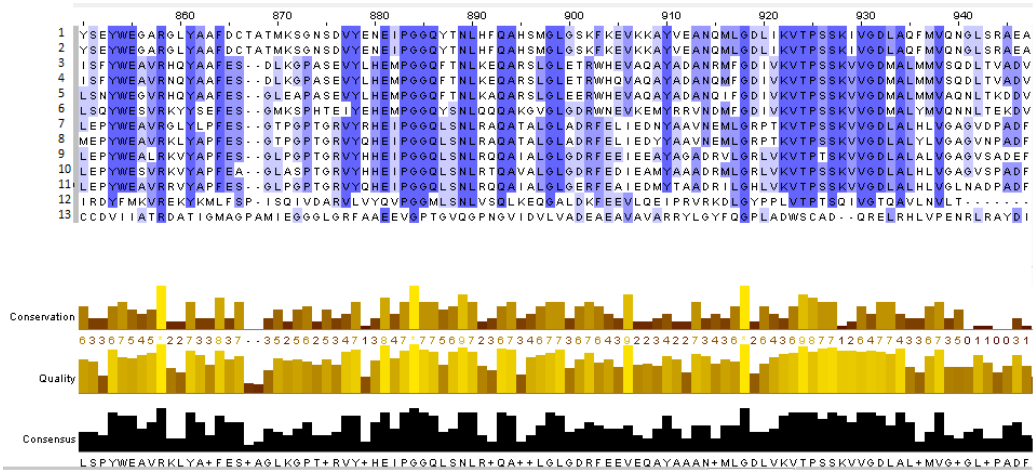

Figure 4. 16 – ClustalW alignment result on carboxylase region. 1-*Homo sapiens;2-Mus musculus;3-Methanocaldococcus jannashii;4-Bacillus Subtilis;5-Rhodobacter capsulatus;6-Sinorhizobium meliloti;7-Corynebacterium glutamicum;8-Asthrobacter globiformis;9-Corynebacterium diphtheria;10-Pseudomonas aeruginnosa;11-Mycobacterium tuberculosis;12-Rhizobium etli;13-Streptomyces coelicolor*

PFam also identified an HGML-like domain in PCx from Streptomyces and so this domain was also compared with those described in other PCxs. The result obtained does not show such high conservation levels as those obtained in the analysis of the above referred domains, however, it seems that indeed *S. coelicolor* PCx belongs to the HGML-family of proteins (Figure 4.17).

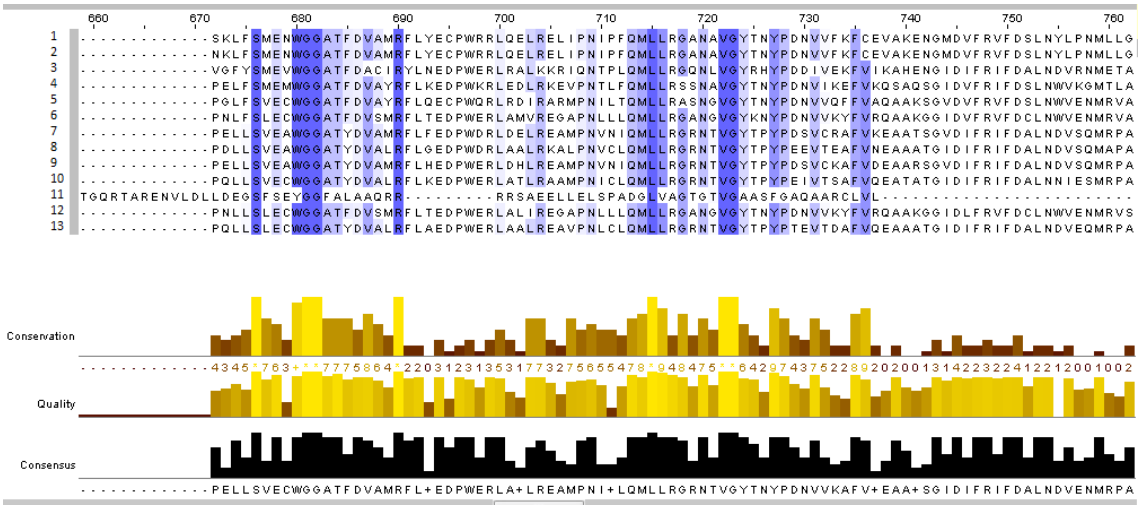

Figure 4. 17 – ClustalW alignment result on HMGL-like region. *1-Homo sapiens;2-Mus musculus;3-Methanocaldococcus jannashii;4-Bacillus Subtilis;5-Rhodobacter capsulatus;6-Sinorhizobium meliloti;7-Corynebacterium glutamicum;8-Asthrobacter globiformis;9-Corynebacterium diphtheria;10-Pseudomonas aeruginnosa;11-Mycobacterium tuberculosis;12-Rhizobium etli;13-Streptomyces coelicolor*

This same alignment allowed the construction of the neighbour-joining tree which by analysing Figure 4.18 revealed some more aspects of the similarity of enzyme of *S. coelicolor* PCx enzyme with those of other organisms. From the built neighbour-joining tree, one of the most notorious aspects is the broad selection of organism presented. The selection made ranges from *P. aeruginosa* to *H. Sapiens* (see Table 3.13 in **chapter 3.10 Bioinformatic analysis**). This indicates how relevant this enzyme is to the organisms' metabolism, which is not surprising considering its metabolic positioning. The selected organisms to align were some of the ones who had their Pyruvate carboxylase characterised before plus some other organism considered relevant to this work. In this figure it possible to see the formation of two distinct groups comprised with *S. coelicolor, M. tuberculosis A. globiformis* and both *Corynebacterium* species, and the other one with *S meliloti*, *R. etli , R. capsulatus, B. subtilis* and finally mouse and human species. Also there are two organisms slightly more distant from the rest of the group, *M. jannaschii* and P. *aerugionsa*.

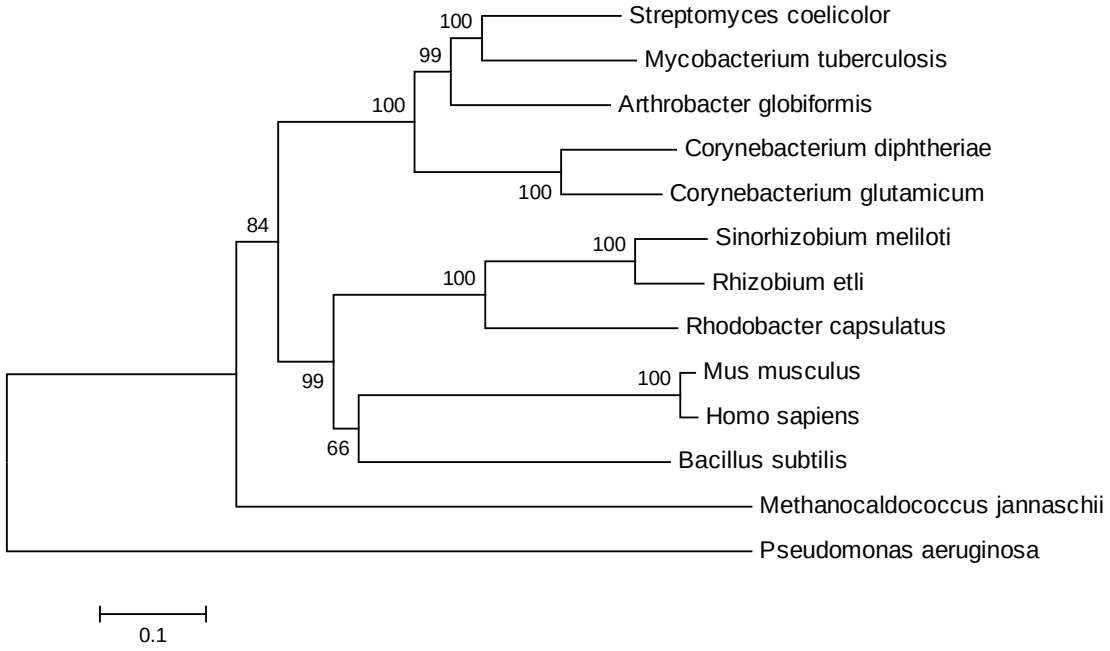

Figure 4. 18 – Neighbor-joining tree Alignment

The formation of major two groups is a logic response if one bears in mind the taxonomic arrangement. The first five organisms are all members of Actinobacteria phylum, therefore some similarity is expected when compared with the members of other phyla. Nevertheless it is remarkable how conserved this enzyme is within the Actinobacteria phylum suggesting an important role. On the second group, containing human and mouse PCxs it is interesting to note how *B. subtillis* enzyme is closer to the higher organisms PCx than to the rest the microorganisms. Sinorhizobium and Rhizobium belong to the same genus and therefore a highly likelihood is expected but *Rhodobacter capsulatus* which is from the same class of *P. aeruginosa* are not as close as expected which is intriguing, however the annotated sequence for *P. aeruginosa* has not been confirmed yet remaining as a putative enzyme.

At last it was also aligned the PCx from an Archaea member, M. *jannaschii*, although it is one of the less similar enzymes, it is very interesting the fact that it exists in this domain confirming how well spread is PCx and how important anaplerosis is for the microorganisms.

Using the insights gathered from the in sillico analysis of S. coelicolor PCx a biochemical characterization of the protein was envisaged in this work. For this, the gene encoding this enzyme was cloned in a controlled expression vector (pET100) and over-expressed in *E. coli*. The first step of this cloning experiment was to amplify the fragment of interest by PCR following the experimental conditions detailed in section **3.7.1. Polymerase Chain Reactions Experiments**. The figure below depicts a typical result of the PCR experiments carried out.

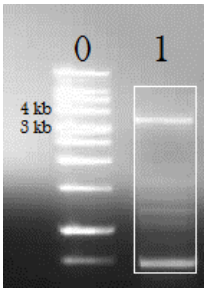

Figure 4.19 – Gel electrophoresis PCR on SCO546 for over expression. 0 – 1 kb Promega ladder; 1- Amplified fragment

The amplified fragment has the expected size (3.375 bp) and was used for subsequent cloning into the pET100 D-TOPO vector resulting on the plasmid described on picture 4.20. The primers used to amplify PCx gene were designed to include in the forward primer a CACC sequence to ensure the correct orientation upon the cloning process since the overhang present in the cloning vector (GTGG) allows a suitable attachment to the 5′ end of the PCR product and stabilizes it in the correct orientation.

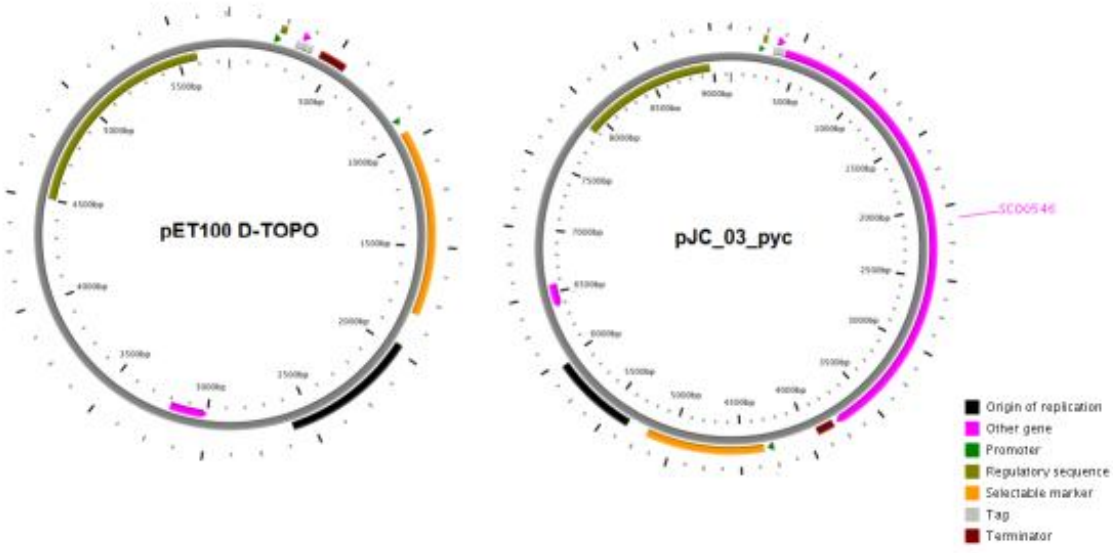

Figure 4.20- Vector map for Plasmid pET100 D-TOPO and pJC_03_pyc

The vector pET100 D-TOPO uses elements from the bacteriophage T7 promoter to express heterologously genes in *E.coli*. T7 RNA polymerase specifically recognizes this promoter therefore it is necessary to deliver T7 RNA polymerase to the cells by inducing expression of the polymerase or infecting the cell with phage expressing the polymerase. In this case Isopropyl β-D-1-thiogalactopyranoside (IPTG) was used to trigger the transcription of lac operon to induce the overexpression of T7 which will overexpress the protein on pET100 TOPO vector[80]. The vector used in this work also allows the C-terminal tagging of the protein of interest with a six histdines tail, which turns possible a purifications step using immunoaffinity chromatography with a metal-chelating resin as the stationary-phase (HisTrap FF).

A simulation of a double digestion of the plasmid pET100 with the PCx gene inserted with *Eco*RV and *Pst*I suggested that the use of these two enzymes should yield DNA fragments with the sizes described on Table 4.6.

Table 4. 6 – Fragments resulting from pJC_03_pyc digestion

Fragments size (bp)	Enzymes Used
4909	EcoRV
3285	PstI
945	

Plasmid DNA of some of the clones obtained was extracted and digested with these two restriction enzymes giving the results that are shown in figure 4.21.

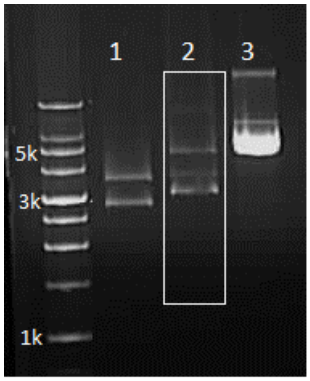

Figure 4. 21 – Gel electrophoresis of pJC_03_pyc::Tn5062digestion with EcoRV and PstI. 0 – 1 kb Promega ladder; 1 – sample digestion; 2-pJC_03_pyc digestion; 3-Undigested pJC_03_pyc

The band pattern obtained differs from what was predicted by the in sillico analysis indicating that the clone in use was not the correct one. To verify such fact the plasmid was sent for sequencing. The results obtained are summarized in Table 4.7.

Table 4. 7 – Alignment score of pJC_03_pyc with M145 Genome	
T7 RNA polymerase promoters	
Score	1830 bits (923)
Identities	970/978 (99%)
Gaps	7/978 (0%)

On Table 4.7 an alignment of the sequenced fragment with M145 genome shows that the fragment inserted correspond to half the PCx gene, that is, instead of holding the complete gene the clone only had a fragment with 1231 bp of the total 3375 bp. The domains of the protein that are produced by these truncated version of PCx clone were analysed in sillico using PFam and the results obtained are described on Figure 4.22 [56].

Figure 4.22 – Pyruvate carboxylase domains according to PFam with the encoded part by pJC_03 (blue box)

This analysis showed that the gene sequence cloned in the pJC_03_pyc vector encoded solely the last carboxylase domain, the HMGL-Like domain and the biotin attachment domain (blue box on Figure 4.17) reducing the expected size of the protein from 120 KDa to a predicted size of 31kDa.

Figure 4.23 – Prediction protein tertiary structure of cloned fragment on pJC_03 (left) and complete structure of PCx in *S. coelicolor* (right)

This image also shows a prediction of the full enzyme to facilitate the comparison between the expected protein and one actually obtained.

Although the fragment cloned allows translation of the carboxylase domain and the biotin attachment domain, it does not allow translation of the carbamoyl phosphate synthetase and the biotin carboxylase carrier domain which are both indispensable for the carboxylation of pyruvate. During the time of this work it was not possible to obtain a clone expressing the full length PCx so it was decided to move on with the biochemical characterization of the truncated protein already obtained. One important information that may come from this analysis is to see if the two domains missing in this truncated form of *S. coelicolor* PCx are indeed required for full protein function. For this, the pJC_03_pyc plasmid was transformed into *E. coli* BL21, over-expressed and subsequently purified. On picture 4.17 It is possible to analyse the chromatogram obtained from the purification procedure. The truncated protein eluted at a volume of 134 mL. The other peak registered later on corresponds to the imidazole present in the buffers used for elution.

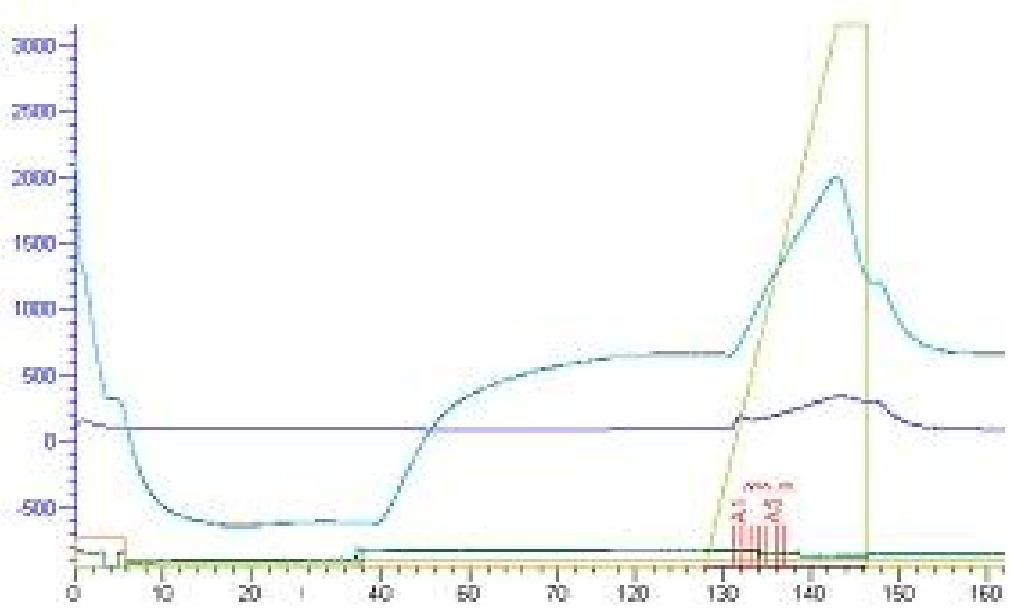

Figure 4. 24 – Chromatogram obtained from the purification of the PCx over expressed by E.coli BL21 transformed with pJC_03

On Figure 4.25 it is depicted an SDS-PAGE with the result obtained before and after the purification step. In lane 4, corresponding to cell debris, it is possible to see a band with around 31 kDa which is presumed to be the truncated PCx protein. Furthermore, a very faint band with the same molecular weight is also present on the third purified sample, lane 8.

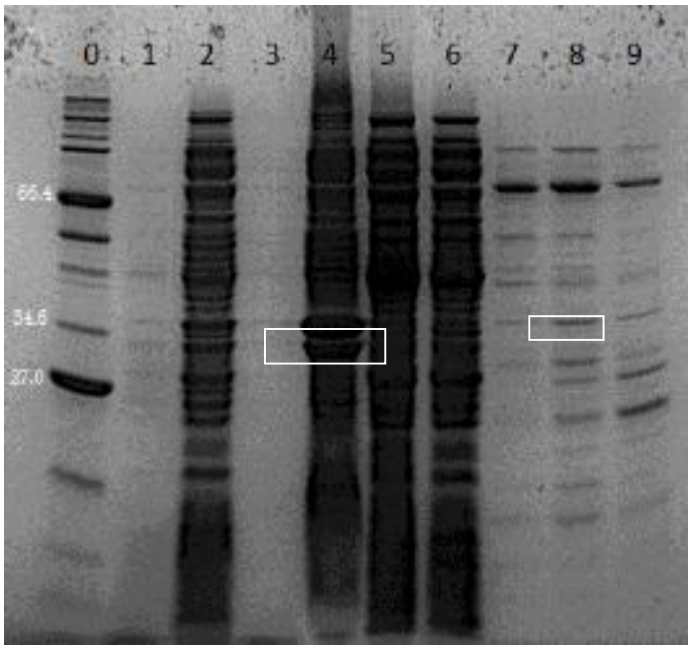

Figure 4.25- SDS page gel with samples taken from overexpression and purification steps. 0 – 2-212 kDa NEB protein Marker; 1 – Cell pellet after induction; 2 – Supernatant After Induction; 3 – Cell Pellet Before Induction; Lane 4 – Cell Debris; 5 – Flow through; 6 – Wash;7 – Purified Sample 1;8 – Purified Sample 2;9 – Purified Sample 3.

The fact that the expected band is mainly on cell debris lane indicates that the protein over-expressed is being accumulated in inclusion bodies. Indeed, inclusion bodies are known to be used by E. coli cells to trap misfolded or inactive protein versions [81].

Since an experimental protocol was not available to assay the activity of *S. coelicolor* PCx this was carried out in this work. The main reactions behind this experiment were described by DeForchetti and Cazzulo, 1975, [82] and are shown below as reaction (3) and (4).

$$Pyruvate + ATP + HCO_3^- \longrightarrow Oxaloacetate + ADP + P_i \quad (3)$$

$$Oxaloacetate + NADH \longrightarrow Malate + NAD^+ \quad (4)$$

Reaction 3 is catalysed by pyruvate carboxylase while the oxidation of NADH in the OAA transformation to malate is catalyzed by malate dehydrogenase (Reaction 4). In this case the activity of the enzyme was followed through the decrease of NADH absorbance at 340 nm and one unit of PCx was defined by the oxidation of 1 µmol NADH per minute. To assess the conditions for the enzyme assay, experiments were conducted at different pHs and temperatures. These assays were carried out using whole-cell *S. coelicolor* extracts.

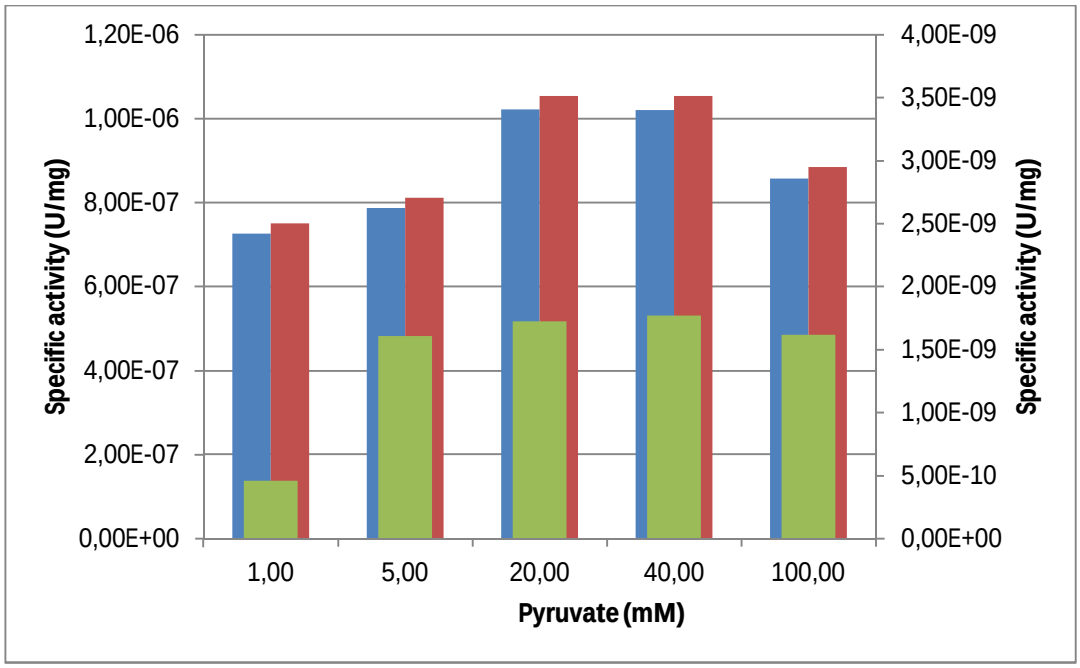

Figure 4. 26 - – Plot resulting from the condition analysis for the enzymatic assay performed to a cell extract of Wild type; Red - pH7 at Room Temperature; Blue - pH 7 at 30ºC; Green - pH 8.5 at Room temperature (right YY axis)

The results obtained show that at higher pHs (pH 8.5) drastically reduces S. coelicolor PCx activity reaching a maximum value of $2.25x10^{-9}$ U/mg. At pH 7 at 30ºC and room temperature the activity reached $1.02x10^{-7}$ U/mg and $1,05x10^{-7}$U/mg. Based on these results it was found that *S. coelicolor* PCx enzyme has an optimum pH of 7 and an optimum temperature around 25ºC (room temperature). Using this experimental protocol it was possible to have tested whether the purified truncated protein had PCx activity which was confirmed to be inactive and to perform primary characterization of the enzyme and comparing it to the mutant (Figure 4.27).

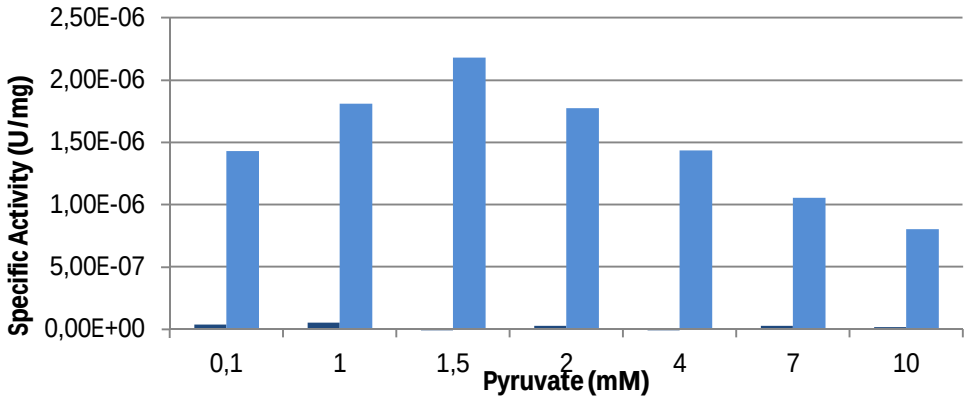

Figure 4. 27 – Plot resulting from the enzymatic assay performed to a cell extract of Wild type (Light blue) and M145Δpyc::Aac(3)IV (dark blue)

One striking feature of Figure 4.27 is the decrease registered in the activity that was observed for increasing pyruvate concentrations. This substrate inhibition is controversial with the previous evidence regarding growth on solid media with pyruvate as carbon source. Since previous work had documented this inhibition and this was registered more than one time during the optimisation of this assay, it is possible that the differences registered on solid media could be due to the natural variability of *Streptomyces* strains.

.

5. Discussion

After introducing all the results (see chapter **4. Results**) it is important to interpret what has been done. In this section a critical view of the achieved results will be presented relating those with some of the theoretical background. Upon the creation of the M145Δpyc::Tn5062 mutant the first presented assay was the growth of the strains on solid media. In this case it was assayed the adaptability of the strain to grow with different carbon sources in comparison to the wild-type.

Based on the registered phenotypic differences, some hypotheses were created to explain the strains behaviour. These explanations are hypothetical and require more data to be confirmed.

The first carbon source was acetate. The ability to use this molecule as a carbon source is usually related to the glyoxylate shunt and capacity of the organism to maintain anapleurotic and gluconeogenic functions through two carbon molecules. Moreover, the carbon backbone of a polyketide results from a sequential condensation of short fatty acids such as acetate. [38, 83]

The first conclusion from this assay is that the capacity to activate the glyoxylate shunt has not been compromised, however there is a difference in both strains. A closer look to the organism's metabolism shows that using acetate as a carbon source will diminish the usage of glycolysis pathway thus lowering the concentration of pyruvate, forcing the cell to use more acetyl-CoA to supply the TCA cycle.

Adding to this situation the blockage of the PCx reaction will increase the consumption of acetyl-CoA to anaplerotic functions and consequently making it less available to the PKS system lowering the production of actinorhodin as it can be verified on Figure 4.3. Figure 5.1 illustrates what has been explained previously.

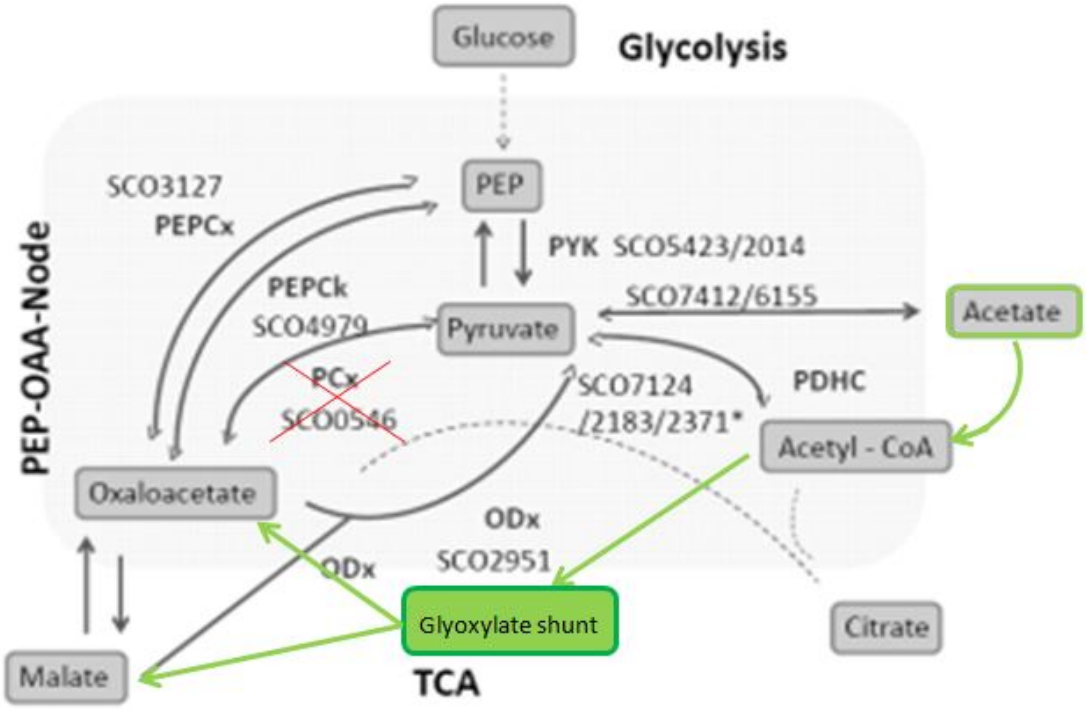

Figure 5. 1 – Possible effects on the carbon flux in M145Δpyc::Tn5062 when using acetate as a carbon source in minimal medium

On the second image of Figure 4.3, citrate was used as carbon source. In this case the wild type presents a higher concentration of Act than the mutant. The explanation found for this fact relies on the role of citrate in the organism metabolism, being an intermediate of Krebs cycle confers an anaplerotic role to this molecule that may attenuate the impact of SCO0546 knockout, leaving the difference between both strains to a slower growth rate of M145Δpyc::Tn5062. Hence the presence of Red as the mutant is due to the fact that is still in a previous growth stage. Figure 5.2 describes a possible metabolic route for citrate that could be an explanation for the observed phenotype.

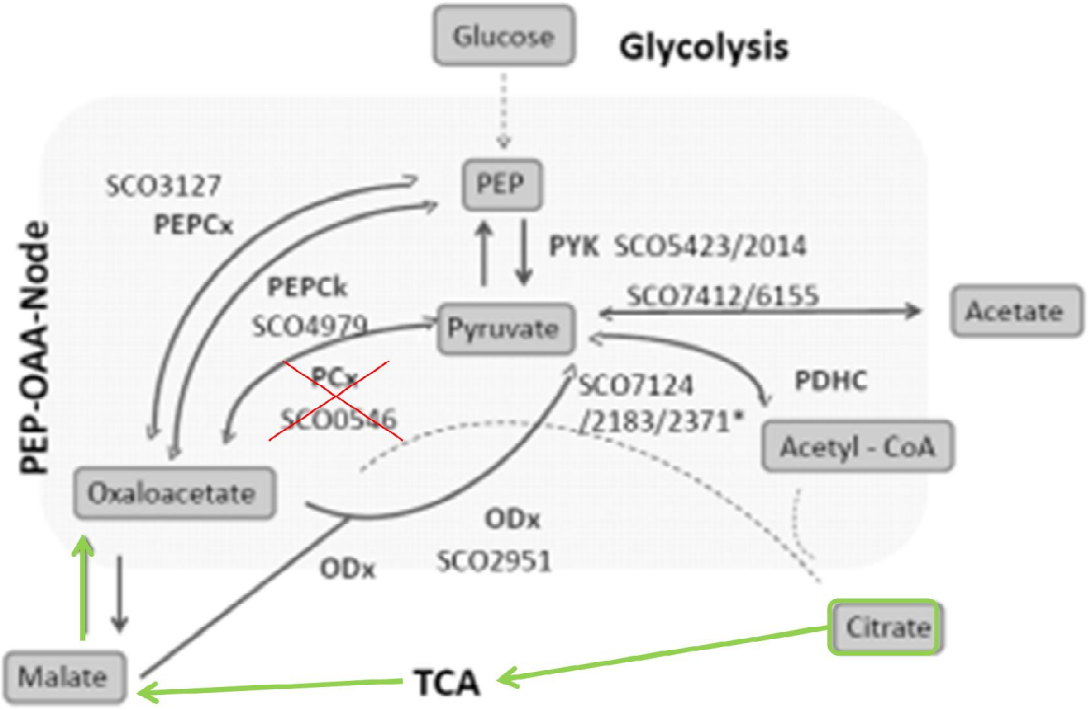

Figure 5. 2 – Possible effects on the carbon flux in M145Δpyc::Tn5062 when using citrate as a carbon source in minimal medium

As Figure 5.3 shows, supplying the microorganism with pyruvate offers the cell a greater flexibility on its metabolism when compared to carbon sources like acetate. From pyruvate it is possible to supply the TCA cycle or initiate gluconeogensis more easily. In this case the mutant presents a higher production of actinorhodin when compared with the wild type (Figure 4.3).

The increased production of actinorhodin can be explained by an augmentation of the amount of acetyl-CoA in the cell. Once again the blockage of PCx reaction unbalances the consumption of pyruvate and this fact is aggravated in a situation where this substrate is in excess. Therefore by not being able to carboxylating pyruvate into OAA, M145Δpyc::Tn5062 may use it to form more acetyl-Coa inducing the formation of actinorhodin by the PKS system.

Later in this work it was shown that pyruvate carboxylase presents some substrate inhibition, data that would be conflicting with this explanation, however using pyruvate as sole carbon source in solid media is a different environment from the one where the substrate inhibition was registered.

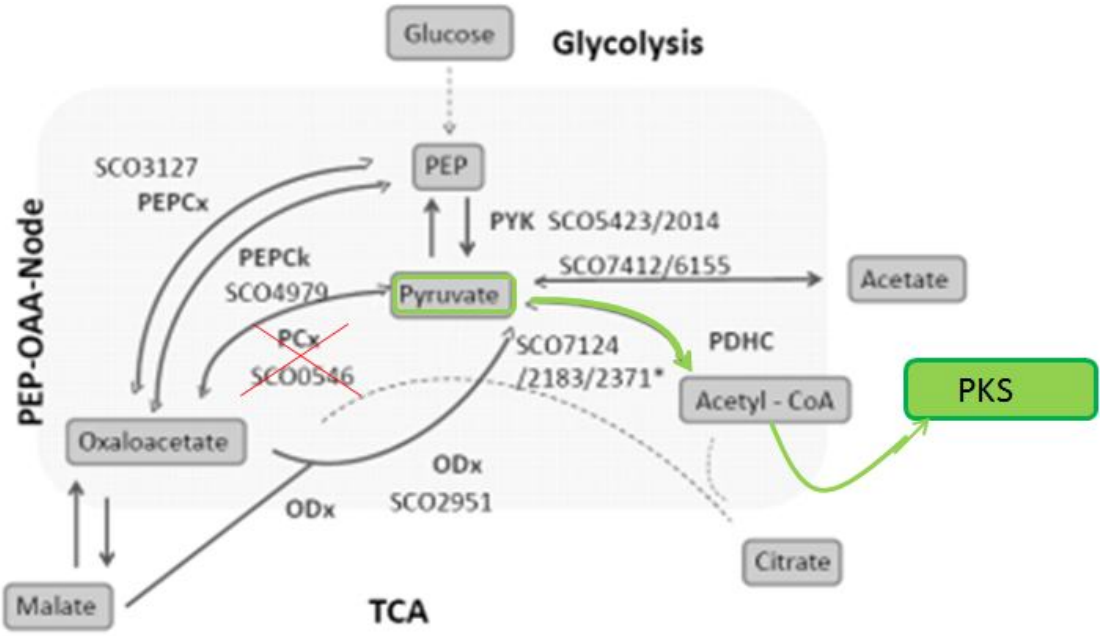

Figure 5.3 – Possible effects on the carbon flux in M145Δpyc::Tn5062 when using pyruvate as a carbon source in minimal medium

N-Acetylglucosamine (GlcNAc), is a favoured carbon and nitrogen source for Streptomycetes however it has other functionalities such as blocking or triggering secondary metabolism and antibiotic production depending if it is growing on rich or minimal media [29]. Furthermore, GlcNAc is known to be involved in the phosphotranferase system, in fact it has been proven that in *S. coelicolor* prefers to use GlcNAc in this system. It was also proven that some Streptomycetes rely on a phosphoenol-dependent phosphotransferase system for the uptake of GlcNAc [84].

In this case the concentration of GlcNAc used seems to have decreased the antibiotic production on wild type however it can be verified that M145Δpyc::Tn5062 has a slightly higher antibiotic production. Knowing that the uptake of GlcNAc is PEP dependent and the conversion of PEP into pyruvate yields one molecule of ATP it is possible to assume that an increase of PEP, to help incorporating GlcNac, may reflect in an increase of pyruvate as well. The blockage of pyruvate to oxaloacetate reaction may induce the increase of acetyl-CoA which is the starter molecule for the PKS and consequently to actinorhodin production. Figure 5.4 supports the explanation presented previously.

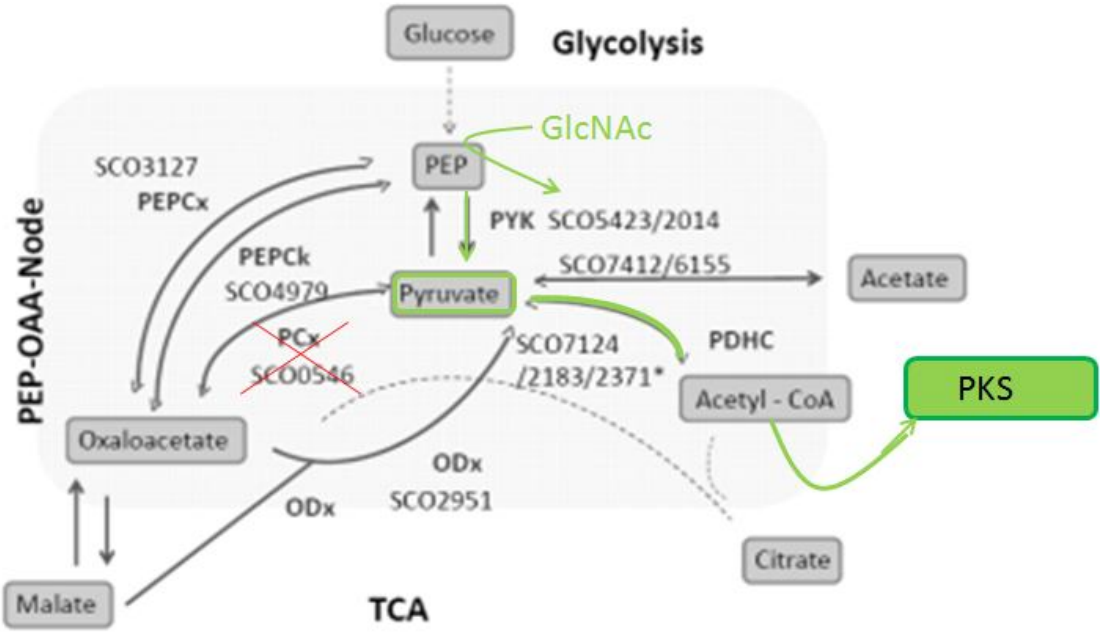

Figure 5.4 – Possible effects on the carbon flux in M145Δpyc::Tn5062 when using GlcNAc as a carbon source in minimal medium

Another carbon source tested was tween 80. Being structurally similar to fatty acids, it will be metabolised through the fatty acid pathway, which feeds relatively quickly into acetyl-CoA, a polyketides molecule precursor, hoping that such fact would reflect in a higher antibiotic production yield. However there was no phenotypic difference between mutant and wild type [85].

In this case, organism should obtain acetyl-CoA mainly through the degradation of tween therefore the influence of PCx in the metabolism is diminished meaning no differences would be registered between wild type and mutant.

Using glucose as a carbon source diminished the antibiotic production in M145Δpyc::Tn5062. In this particular case, inhibiting the PCx reaction may have had a greater impact on the strains development then on its capacity to produce antibiotic production. Thus the differences registered are due to a slower growth rate from the mutant which may not have reached the secondary phase yet.

The elations made in this case are not corroborated with further experiments in liquid media however, because the conditions are not the same it is not possible to ensure that this phenotype is solely due to a slower growth rate or the inherent Streptomycetes variability took part in this assay. Moreover the fact *S.coelicolor* is being grown in liquid media alters their life cycle as they do not sporulate which might also have an influence on the organism metabolism[23, 24].

The same strains were also grown on four types of rich media, however, in this case, there were no significant differences. Figure 2.13 shows how Act and Red production were not compromised as well as sporulation process. This fact is a good indicator that in good growth conditions PCx inhibition can be overcome possibly due to the presence of PEP carboxylase.

The first presented assay in liquid media was a high throughput experiment. The data showed some variation (Figure 4.5) which may result from the inherent variability of Streptomycetes or due to the experiment conditions. During this experiment some problems regarding evaporation of the media had to be dealt with, and although the use of a plastic membrane seemed to solve the problem on the majority of the wells, a few of them had a significant volume decrease by the end of the experiment.

Moreover as it was an experiment in liquid media spore formation and aerial hyphae were not expected, however at least one of the wells presented those development stages (Figure 4.5 – Well C3, C4). This fact may result the small volume inoculated which may had offered enough surface tension to hold a development of aerial hyphae and consequently spore formation.

Nevertheless, Figure 4.6 translated what can be seen on Figure 4.5 into numbers which corroborate the already presented explanation of the M145Δpyc::Tn5062 slower growth rate as both mutants present a smaller amount of biomass.

On the other hand, actinorhodin concentration is higher which is controversial to what is shown in the solid media assay, nevertheless these results were obtained constant through all the five well with a relatively lower error bars. Moreover a second experiment in liquid media corroborated these results. Therefore, it possible to say a blockage of PCx may result in an increase of acetyl-CoA which may lead into a higher production of polyketides, namely actinorhodin.

Besides in liquid media the organism is affected to all new kinds of stress such as the oxygen transfer issue and the availability of certain nutrients, which may run lower than on solid media. Moreover the fact that in the end of the experiment the final volume was not equal may had had an influence too as evaporation might be a stressful event interfering with the antibiotic production. All of these factors will contribute to a different response between both media.

The second experiment in liquid media was growth curve in this case the results obtain in the 24-well plate were corroborated as it is possible to verify that the biomass is slightly lower in the mutant and its actinorhodin production was doubled.

It is also noteworthy that the antibiotic was only produced in the stationary phase as mentioned in literature review, showing that, although the carboxylation of pyruvate takes part on the central carbon metabolism, the antibiotic production is not anticipated during the exponential phase.

The bioinformatic analysis demonstrated the similarities between this enzyme and other PCxs which supports the expectation of a similar behaviour regarding inhibitions or enhancements of the proteins activity.

Regarding the enzyme characterisation a new clone need to be achieved to in order to be able to study the biochemistry of the reaction. As Figures 4.22 and 4.23 show, the enzyme is not complete. Still because the carboxylase domain was present it was decided to still verify if the protein showed any activity thus proceeding with the overexpression and purification protocols

Although the purified samples were not active, the fact that the concentration of the protein in study was not as high as desired (having some other bands with a stronger presence than the one with the expected size) does not permit to conclude the carbamoyl phosphatase domain is indeed indispensable. However this not expected as this is not a favourable reaction and the activation of the carboxyl group is indeed necessary.

The enzyme characterisation with cell extract demonstrated a substrate inhibition which is consistent with previous work in other PCx. From a metabolic point of view this inhibition is a very sharp method from the bacteria to give other uses to pyruvate, as blocking this activity would leave more pyruvate to be used in other routes such as acetyl-CoA formation (the starter molecule for the FAS and PKS system, for instance).

Although the assay was already insightful about PCx characteristics it would have been interesting to look for some the effect of other molecules such as ADP or AMP, as well as some other TCA cycles intermediates like malate or citrate and investigate if the presence of those molecules would inhibit or activate PCx activity.

Although this issue was not studied it was expected (by comparing with PCx from other organisms) that AMP or ADP would inhibit this enzymes activity, which make some sense as in a presence of many molecules of ADP and ATP it is accepted some wise usage of the lower amount of ATP[59-61]. Moreover molecules like citrate and malate in excess could offer other possibility to form OAA facilitating other uses for pyruvate.

This work was a contribution to PhD project to characterise the complete PEP-PYR-OAA node towards achieving better antibiotic yields. By characterising the knockout mutant and the protein involved in the particular reaction of pyruvate carboxylation, we are now one step closer to fully understand this metabolic switch.

Some of the data generated, such as the growth curve on glucose as carbon source, showed that M145Δpyc::Tn5062 is a better actinorhodin producer than the wild type, producing two times more Act. Furthermore the growth with different carbon sources shed some light on the metabolic routes creating some room to generate hypothesis on how *S. coelicolor* metabolism works under given conditions.

The enzymatic characterisation settled some grounds to fully characterise the reaction itself by creating a protocol to work with this protein. Moreover some of the experiments done granted some knowledge of what is at stake when it comes to carboxylate pyruvate into oxaloacetate such as the substrate inhibition.

Although some knowledge was obtained with this work, it would have been relevant to complement the mutant and purify the protein in order to confirm some of the hypothesis created. Nevertheless the obtained results already point towards the relevance of this enzyme in the organism.

As future remarks, at short-term, it would have been relevant to characterise the mutant in different carbon sources in liquid media and study the organism's response. From the enzymatic point of view it could be relevant to study the effect of molecules like ADP, OAA, PEP and acetyl-CoA on the enzyme's activity.

As long-term objectives it will be interesting to combine the knowledge form all the other reactions and achieve deeper knowledge of the PEP-PYR-OAA Node and eventually create a better antibiotic producer strain.

6. References

1. Davies, J. and D. Davies, *Origins and evolution of antibiotic resistance.* Microbiol Mol Biol Rev, 2010. **74**(3): p. 417-33.
2. Butler, M.J., et al., *Engineering of primary carbon metabolism for improved antibiotic production in Streptomyces lividans.* Appl Environ Microbiol, 2002. **68**(10): p. 4731-9.
3. Watve, M., et al., *How many antibiotics are produced by the genus<SMALL> Streptomyces</SMALL>?* Archives of Microbiology, 2001. **176**(5): p. 386-390.
4. Akagawa, H., M. Okanishi, and H. Umezawa, *A plasmid involved in chloramphenicol production in Streptomyces venezuelae: evidence from genetic mapping.* J Gen Microbiol, 1975. **90**(2): p. 336-46.
5. Borodina, I., P. Krabben, and J. Nielsen, *Genome-scale analysis of Streptomyces coelicolor A3(2) metabolism.* Genome Res, 2005. **15**(6): p. 820-9.
6. Hopwood, D.A.C., K.F.; Dowding, J.E.; Vivian A., *Advances in Streptomyces coelicolor genetics.* Bacteriol Rev., 1973 **37**(3): p. 35.
7. Sauer, U. and B.J. Eikmanns, *The PEP-pyruvate-oxaloacetate node as the switch point for carbon flux distribution in bacteria.* FEMS Microbiol Rev, 2005. **29**(4): p. 765-94.
8. Petra G. Peters-Wendisch, V.F.W., Susanne Paul,Bernhard J. Eikmanns, Hermann Sahm, *Pyruvate carboxylase as an anaplerotic enzyme in Corynebacterium glutamicum.* Microbiology 1996. **143**(4): p. 8.
9. Singh, S.B. and J.F. Barrett, *Empirical antibacterial drug discovery—Foundation in natural products.* Biochemical Pharmacology, 2006. **71**(7): p. 1006-1015.
10. Okamoto, S.T., T.; Ochi, K.; Ichinose,K., *Biosynthesis of Actinorhodin and Related Antibiotics: Discovery of Alternative Routes for Quinone Formation Encoded in the act Gene Cluster.* Chemistry & Biology, 2009. **16**(February): p. 11.
11. White, J. and M. Bibb, *bldA dependence of undecylprodigiosin production in Streptomyces coelicolor A3(2) involves a pathway-specific regulatory cascade.* J Bacteriol, 1997. **179**(3): p. 627-33.
12. Hobbs, G., et al., *An integrated approach to studying regulation of production of the antibiotic methylenomycin by Streptomyces coelicolor A3(2).* J Bacteriol, 1992. **174**(5): p. 1487-94.
13. Hojati, Z., et al., *Structure, biosynthetic origin, and engineered biosynthesis of calcium-dependent antibiotics from Streptomyces coelicolor.* Chem Biol, 2002. **9**(11): p. 1175-87.
14. Ventura, M., et al., *Genomics of Actinobacteria: tracing the evolutionary history of an ancient phylum.* Microbiol Mol Biol Rev, 2007. **71**(3): p. 495-548.
15. Hopwood, D.A., *Forty years of genetics with Streptomyces: from in vivo through in vitro to in silico.* Microbiology, 1999. **145 (Pt 9)**: p. 2183-202.
16. McCarthy, A.J. and S.T. Williams, *Actinomycetes as agents of biodegradation in the environment — a review.* Gene, 1992. **115**(1–2): p. 189-192.
17. Nothaft, H.F., D.; Wilimek, A.; Mahr, K.; Niederweis, M.; Titgemeyer, F., *The phosphotransferase system of Streptomyces coelicolos is biased for N-acetylglucosamine metabolism.* J Bacteriol, 2003. **185**(23): p. 5.
18. Siebenberg, S., et al., *Reducing the variability of antibiotic production in Streptomyces by cultivation in 24-square deepwell plates.* Journal of Bioscience and Bioengineering, 2010. **109**(3): p. 230-234.
19. Bentley, S.D., et al., *Complete genome sequence of the model actinomycete Streptomyces coelicolor A3(2).* Nature, 2002. **417**(6885): p. 141-7.
20. Chater, K.F., *Regulation of sporulation in Streptomyces coelicolor A3(2): a checkpoint multiplex?* Current Opinion in Microbiology, 2001. **4**(6): p. 667-673.
21. Buttner, M.F., K., *Streptomyces morphogenetics: dissecting differentiation in a filamentous bacterium.* Nature reviews - Microbiology, 2009. **7**(January): p. 15.

22. Clark, L.C. and P.A. Hoskisson, *Duplication and evolution of devA-like genes in Streptomyces has resulted in distinct developmental roles.* PLoS One, 2011. **6**(10): p. e25049.
23. Erikson, D., *Loss of aerial mycelium and other changes in Streptomycete development due to physical variations of cultural conditions.* J Gen Microbiol, 1955. **13**(1): p. 136-48.
24. Karandikar, A.S., G.P.; Hobbs, G., *143.* Microbiology, 1997. **143**: p. 9.
25. Nieselt, K.B., F.;Herbig, A.;Bruheim,P.;Wentzel, A.;Jakobsen, Ø. M;Sletta, H.;Alam, M.T.;Merlo, M. E.;Moore, J.;Omara, W. A.M.;Morrissey, E.R.;Juarez-Hermosillo, M. A.;Rodríguez-García, A.;Nentwich, M.;Thomas, L.;Iqbal, M.;Legaie R.;Gaze, W. H.;Challis, G. L.;Jansen, R. C.; Dijkhuizen,L.; Rand, D. A.;Wild, D. L.; Bonin, M.;Reuther, J.;Wohlleben, W.;Smith, M.C.M.; Burroughs M.C.M.;Martín J.F.; Hodgson, D.A.; Takano, E.; Breitling, R.; Ellingsen, T.E.;Wellington E.M.H.;, *The dynamic architecture of the metabolic switch in Streptomyces coelicolor.* BMC Genomics, 2010. **11**(10): p. 9.
26. van Wezel, G.P. and K.J. McDowall, *The regulation of the secondary metabolism of Streptomyces: new links and experimental advances.* Natural Product Reports, 2011. **28**(7): p. 1311-1333.
27. Bibb, M.J., *Regulation of secondary metabolism in streptomycetes.* Microbiology, 2005. **8**: p. 7.
28. Doull, J.L.V., L. C., *Nutritional control of actinorhodin production by Streptomyces coelicolor A3(2): suppressive effects of nitrogen and phosphate.* Appl Micorbiol Biotechnol, 1990. **32**: p. 6.
29. Rigali, S.T., F.;Barends, S.;Mulder, S,;Thomae, A.W.;Hopwood, D.A.;van Wezel, G.P. , *Feast or famine: the global regulator DasR links nutrient stress to antibiotic production by Streptomyces.* EMBO reports, 2008. **9**(7): p. 6.
30. Elliot MA, T.N., *Building filaments in the air: aerial morphogenesis in bacteria and fungi.* Microbiology, 2004. **7**: p. 7.
31. Chavraburtty, R.B., M., *The ppGpp Synthetase Gene (relA) of Streptomyces coelicolor A3(2) Plays a Conditional Role in Antibiotic Production and Morphological Differentiation.* Journal of Bacteriology, 1997(Sept.): p. 8.
32. Bibb, M., *The regulation of antibiotic production in Streptomyces coelicolor A3(2).* Microbiology, 1996. **142**: p. 9.
33. Wright, L.F. and D.A. Hopwood, *Actinorhodin is a chromosomally-determined antibiotic in Streptomyces coelicolar A3(2).* J Gen Microbiol, 1976. **96**(2): p. 289-97.
34. Hopwood, D.A. and D.H. Sherman, *Molecular genetics of polyketides and its comparison to fatty acid biosynthesis.* Annu Rev Genet, 1990. **24**: p. 37-66.
35. Cerdeño, A.M.B., M.J.; Challis, G.L., *Analysys of the prodiginine biosynthesis gene cluster of Streptomyces coelicolor A3(2): new mechanism for chain initiation and termination in modular multienzymes.* Chemistry & Biology, 2001. **8**: p. 12.
36. Hopwood, D.A., *Genetic contributions to understanding Polyketide Synthases.* Chem. Rev., 1997. **97**: p. 34.
37. Hranueli, D.P., N.;Borovicka, B.;Bogdan, S.;Cullum, J.;Waterman, P. G.;Hunter I.S., *Molecular Biology of Polyketide Biosynthesis.* food technol. biotechnol., 2001. **39**(3): p. 11.
38. Shen, B.H., C.R., *DEciphering the mechanism for the assembly of aromatic polyketides y a bacterial polyketide synthase.* Proc. Natl. Acad. Sci., 1996. **93**(June): p. 5.
39. Kornberg, H.L., *The role and control of the Glyoxylate Cycle in Escherichia coli.* Biochem. J., 1966. **99**(1): p. 12.
40. Diesterhaft, M.D. and E. Freese, *Role of pyruvate carboxylase, phosphoenolpyruvate carboxykinase, and malic enzyme during growth and sporulation of Bacillus subtilis.* J Biol Chem, 1973. **248**(17): p. 6062-70.

41. T. K. Sundaram, C., J. J.;Kornberg, H. L., *Synthesis of Pyruvate Carboxylase from its Apoenzymeand (+)-Biotin in Bacillus stearothermophilus.* Biochem. J., 1970. **122**: p. 7.
42. Chao, Y.-P.L., J. C., *Alteration of growth yield by overexpression of phosphoenolpyruvate carboxylase and phosphoenolpyruvate carboxykinase in Escherichia coli.* Appl Environ, 1993. **59**: p. 423.
43. peters-Wendisch, P.G.W., V.F.; Paul, S.;Elkmanns, B.J.; Hermann S., *Pyruvate carboxylase as an anaplerotic enzyme in Corynebacterium glutamicum.* Microbiology, 1995(143): p. 9.
44. Owen, O.E.K., S.C. Hanson W.H., *The key role of Anaplerosis and Cataplerosis for Citric acid cycle function.* Journal of Biological Chemistry, 2002. **277**(34): p. 4.
45. Kanehisa, M., et al., *KEGG for integration and interpretation of large-scale molecular data sets.* Nucleic Acids Res, 2012. **40**(Database issue): p. D109-14.
46. Petersen, S., et al., *In vivo quantification of parallel and bidirectional fluxes in the anaplerosis of Corynebacterium glutamicum.* J Biol Chem, 2000. **275**(46): p. 35932-41.
47. Utter, M.F. and D.B. Keech, *Formation of oxaloacetate from pyruvate and carbon dioxide.* J Biol Chem, 1960. **235**: p. PC17-8.
48. Mukhopadhyay, B.S., S.F.; Wolfe, R.S., *Purification, Regulation and molecular and biochemical characterization of Pyruvate Carboxylase from Methanobacterium thermoautotrophicum Starin DH.* Journal of Biological Chemistry, 1997. **273**(9): p. 12.
49. March, J.C.E., M.A.; Altman, E., *Expression of an Anaplerotic Enzyme, Pyruvate Carboxylase, Improves Recombinant Protein Production in Escherichia coli.* Appl Environ Microbiol, 2002. **68**(11): p. 5.
50. Walker, M.E.V.D.L.R., M.; Devenish, R.J.; Wallace, J.C., *Yeast pyruvate carboxylase: identification of two genes encoding two isoenzymes.* Biochem. Biophys, 1991. **176**: p. 8.
51. Jitrapakdee, S.W., J.C., *Structure, function and regulation of pyruvate carboxylase.* Journal of Biochemistry, 1999. **340**(1): p. 16.
52. Attwood, P.V., *The Structure and the mechanism of action of Pyruvate Carboxylase.* Int. J. Biochem, 1995. **27**(3): p. 19.
53. Attwood, P.V.W., J.C., *Cheemichal and catalytic mechanisms of the carboxyl transfer reactions in biotin-dependent enzymes.* Acc Chem. Res, 2002. **35**: p. 8.
54. Maurice, M.S.R., L.; Surinya, K.H.; Atwood, P.V.; Wallace, J.C.; Cleland W.W.; Rayment, I., *Domain Architecture of Pyruvate Carboxylase, a Biotin-Dependent Multifunctional Enzyme.* Science, 2007. **317**(1076): p. 4.
55. Gross, J.A.C., N.D.; Uttter, M.F., *Characterization of the subunit structure of pyruvate carboxylae from Pseudomonas citronellolis.* J. Biol. Chem., 1981. **25**(256): p. 7.
56. Punta, M.C., P.C.;Eberhardt, R.Y.;Mistry, J.;Tate, J.;Boursnell, C.;Pang, N.;Forslund, K.;Ceric, G.;Clements, J.;Heger, A.;Holm, L.; and E.L.L.E. Sonnhammer, S.R.;Bateman, A.;Finn, R.D., *The Pfam protein families database* Nucleic Acids Research Database 2012(40).
57. Burge, S., et al., *Manual GO annotation of predictive protein signatures: the InterPro approach to GO curation.* Database, 2012. **2012**.
58. Jitrapakdee, S.M.M.S.R., I.; Cleland, W.W.; Wallace, J.C.; Atwood, P.V., *Structure, Mechanism and Regulation of Pyruvate Carboxylase.* Biochem. J., 2008. **413**(3): p. 42.
59. Modak, H.V.K., D.J. , *Acetyl-CoA-dependent pyruvate carboxylase from the photosynthetic bacterium Rhodobacter capsulatus: rapid and efficient purification using dyeligand affinity chromatography. .* Microbiology 1995 **141**: p. 10.
60. Voegele, R.T., Mitsch, M.J. Finan, T.M. , *Characterization of two members of a novel malic enzyme class.* Biochim. Biophys. Acta 1999. **1432**: p. 30.
61. Dunn, M.F., Araiza, G. and Finan, T.M., *Cloning and characterization of the pyruvate carboxylase from Sinorhizobium meliloti Rm1021.* Arch. Microbiol. , (2001) **176**

p. 8.
62. Islam, M.N.S., S.; Kondo, H., *Construction of new forms of pyruvate carboxylase to assess the alosteric regulation by acetyl-CoA.* Protein Eng. Des. Sel, 2005. **18**: p. 8.
63. Ozimek, P.v.D., R.; Latchev, K.; Gancedo, C.; Wang, D.Y. van der Klei, I.J., *Pyruvate Carboxylase is an essential protein in the assembly of Yeast peroxissomal oligomeric alcohol oxidase.* Mol. Biol. Cell, 2003. **14**: p. 12.
64. Conn, J.E., *The Pigment Production of Actinomyces coelicolor and A. violaceus-ruber.* J Bacteriol, 1943. **46**(2): p. 133-49.
65. Fernández-Martínez, L.T., et al., *A transposon insertion single-gene knockout library and new ordered cosmid library for the model organism Streptomyces coelicolor A3(2).* Antonie van Leeuwenhoek, 2011. **99**(Article): p. 515-522.
66. Bishop, A., Fielding, S.,Dyson, P., *Systematic Insertional Mutagenesis of a Streptomycete Genome:A link Between Osmoadaptation and Antibiotic Prodution.* Genome Res, 2004. **2004**(14): p. 7.
67. Huang, J.S., J.; Molle, V.; Sohlberg, B.; Weaver, D.; Bibb, M. J.; Kao, C. M.; Buttner, M.J.; Cohen, S. N., *Cross-regulation among disparate antibiotic biosynthetic pathways of Streptomyces coelicolor.* Molecular Microbiology, 2005. **58**(5): p. 11.
68. Bertani, G., *Studies on lysogenesis. I. The mode of phage liberation by lysogenic Escherichia coli.* J. Bacteriol., 1951. **62**: p. 8.
69. Hopwood, D.A., *Genetic analysis and genome structure in Streptomyces coelicolor.* Bacteriol Rev, 1967. **31**(4): p. 373-403.
70. Hobbs, G., et al., *Dispersed growth of <i>Streptomyces in liquid culture.* Applied Microbiology and Biotechnology, 1989. **31**(3): p. 272-277.
71. Kieser, T.B., M.J.; Buttner, M.J.;Chater, K.F.;Hopwood, D.A.;, *Practical Streptomyces Genetics*. Vol. 1. 1990, Norwich, England: John Innes Foundation.
72. Strauch, E., et al., *The stringent response in Streptomyces coelicolor A3(2).* Molecular Microbiology, 1991. **5**(2): p. 289-298.
73. Bradford, M.M., *A rapid and sensitive method for the quantitation of microgram quantities of protein utilizing the principle of protein-dye binding.* Anal Biochem, 1976. **72**: p. 248-54.
74. Tamura K, P.D., Peterson N, Stecher G, Nei M, and Kumar S *MEGA5: Molecular Evolutionary Genetics Analysis using Maximum Likelihood, Evolutionary Distance, and Maximum Parsimony Methods.* Molecular Biology and Evolution, 2011
75. Larkin, M.A., et al., *Clustal W and Clustal X version 2.0.* Bioinformatics, 2007. **23**(21): p. 2947-8.
76. Fernandez-Martinez, L.T., et al., *A transposon insertion single-gene knockout library and new ordered cosmid library for the model organism Streptomyces coelicolor A3(2).* Antonie van Leeuwenhoek, 2011. **99**(3): p. 515-22.
77. Flett, F.M., V.; Smith C.P., *High efficiency intergeneric conjugal transfer of plasmid DNA from Escherichia coli to methyl DNA-restricting streptomycetes.* FEMS Microb. Letters 1997. **155**: p. 7.
78. Jyothikumar, V., et al., *Time-lapse microscopy of Streptomyces coelicolor growth and sporulation.* Appl Environ Microbiol, 2008. **74**(21): p. 6774-81.
79. Promega, *pGEM®-T and pGEM®-T Easy Vector Systems Techincal Manual*, P. Corporation, Editor 2010: USA.
80. Quimron, U., *New details about bacteriophage T7-host interactions.* Microbe, 2010. **5**(3): p. 6.
81. Martinez-Alonso, M., et al., *Learning about protein solubility from bacterial inclusion bodies.* Microb Cell Fact, 2009. **8**: p. 4.
82. De Forchetti, S.R.M.C., J. J. , *Some Properties of the Pyruvate Carboxylase from Pseudomonas Jluorescens.* Journal of General Microbiology, 1975. **93**: p. 7.

83. Ensign, S.A., *Revisiting the glyoxylate cycle: alternate pathways for microbial acetate assimilation.* Molecular Microbiology, 2006. **61**(2): p. 3.
84. Wang, F.X., X.; Saito, A.; Schrempf, H., *Streptomyces olivaceoviridis possesses a phosphotransferase system that mediates specific, phosphoenolpyruvate-dependent uptake of N-aacetylglucosamine.* Mol. Genet. Genomics 2002. **268**(3): p. 7.
85. Dalmau, E., et al., *Effect of different carbon sources on lipase production by Candida rugosa.* Enzyme and Microbial Technology, 2000. **26**(9–10): p. 657-663.

Annex

Annex Figure I a Polyketide Synthase system

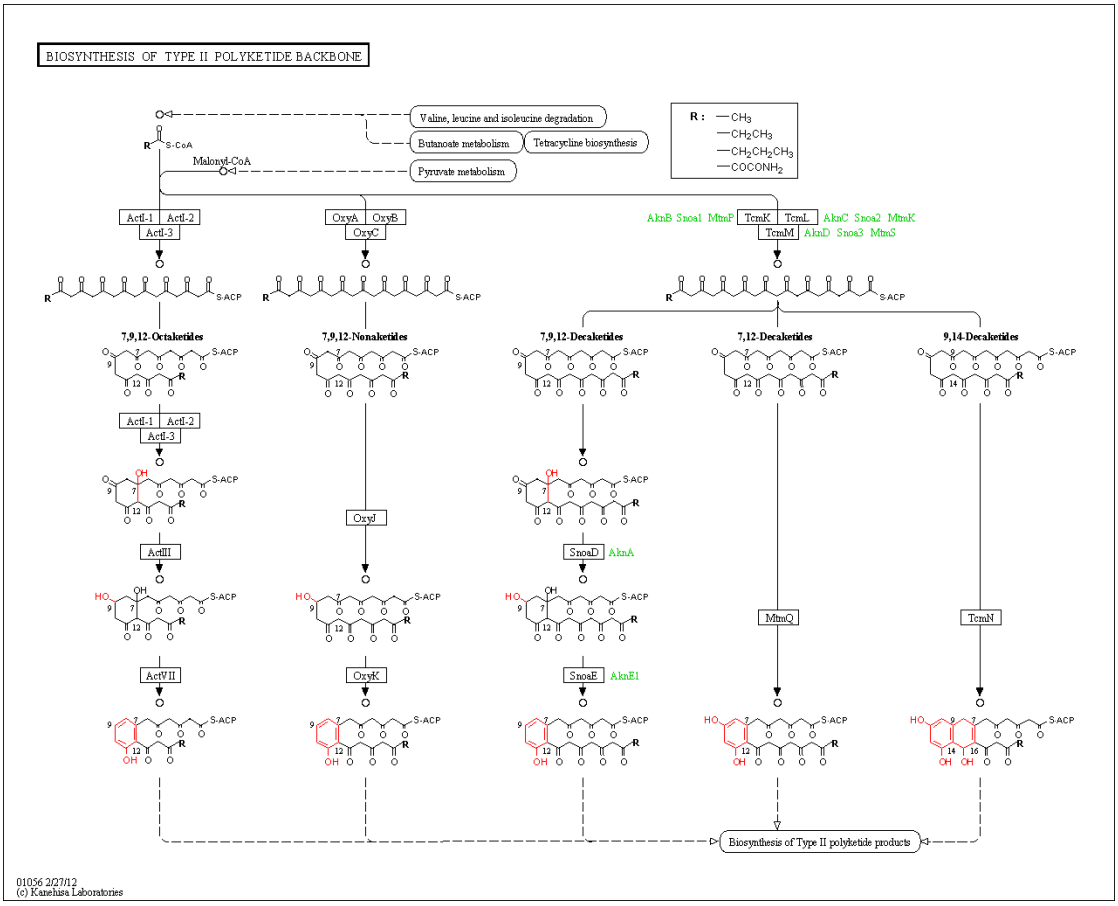

Annex Figure I a Polyketide Synthase system

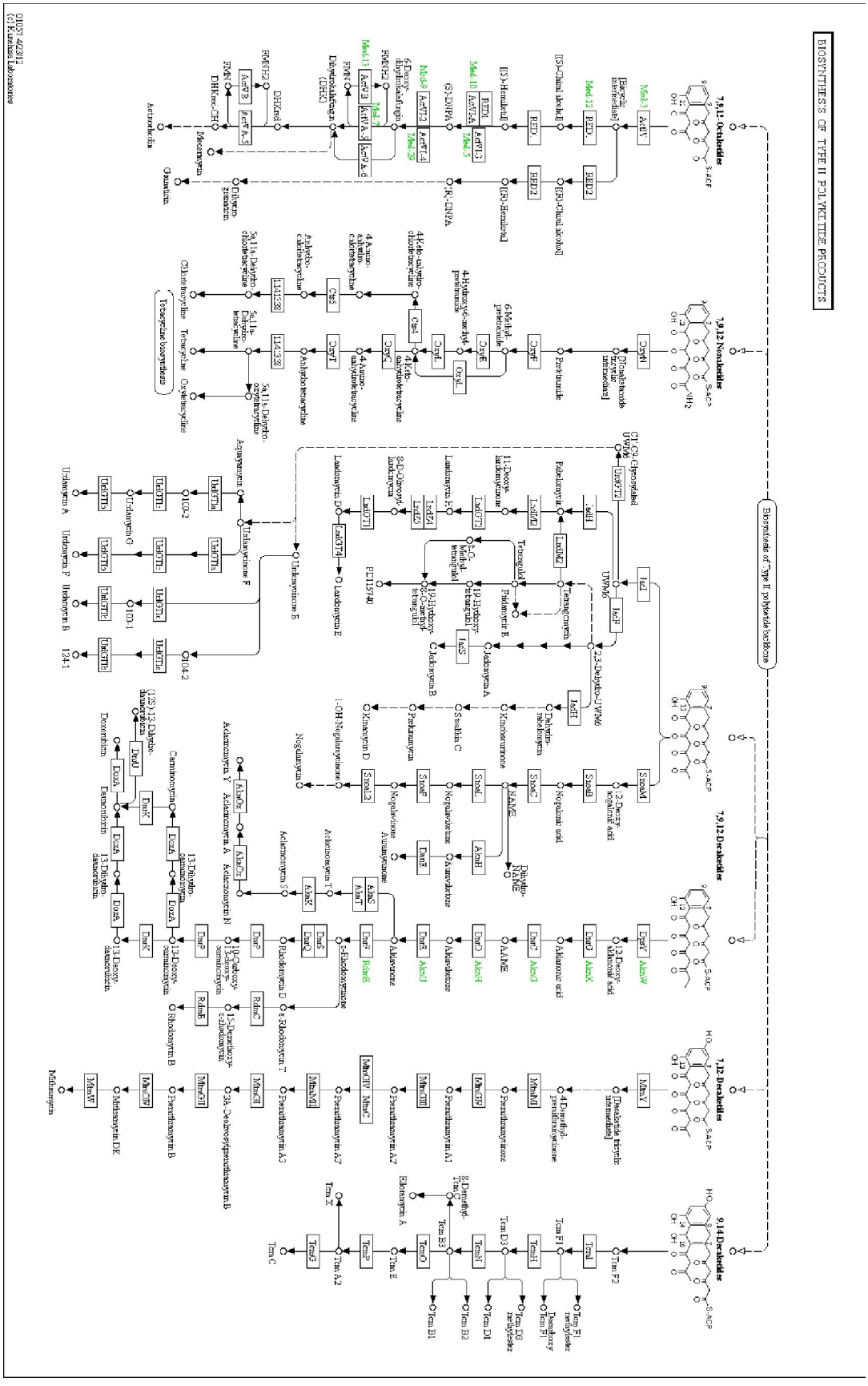

Annex Figure II – Reaction scheme for pyruvate carboxylation by PCx

A

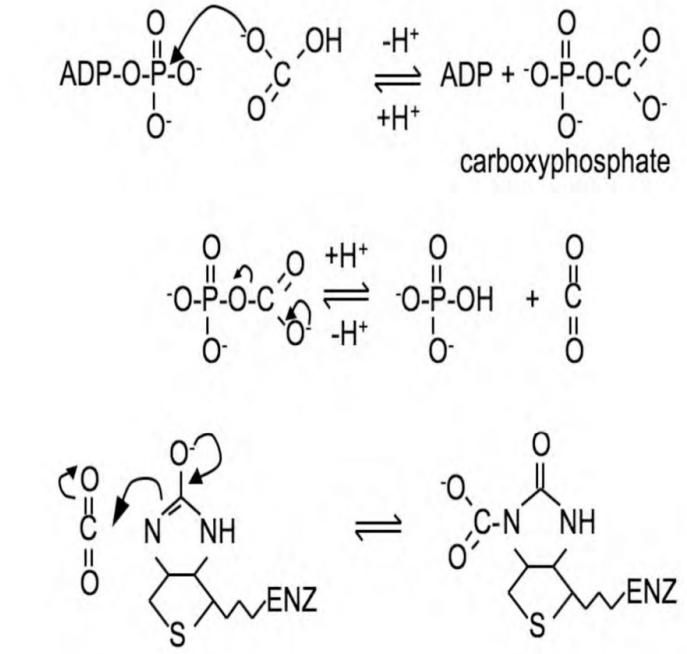

B

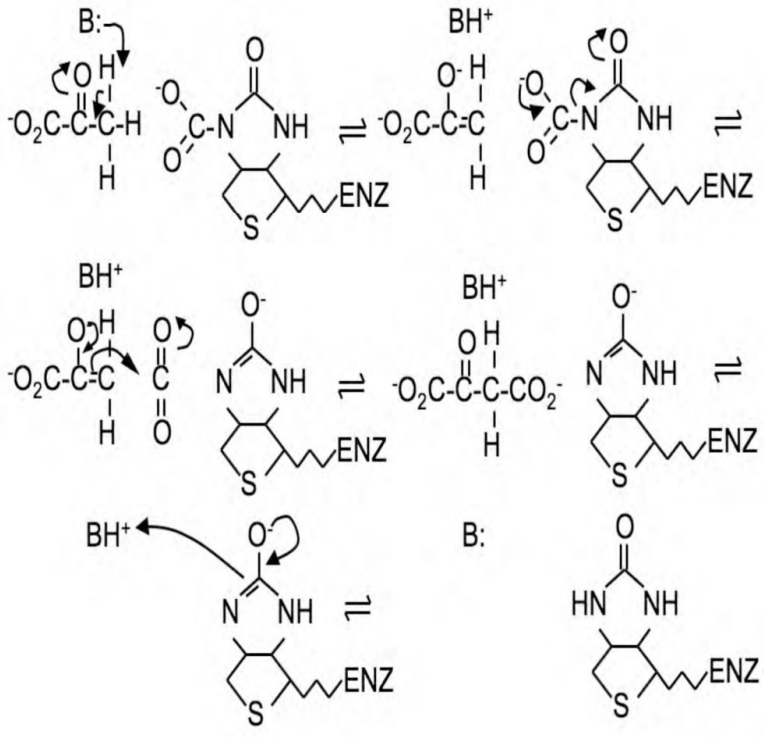

Annex equation AI – Molar ratio Equation

$$Molar\ Ratio_{Insert:Vector} = \frac{kbp_{vector}}{ng_{vector} \times kbp_{insert}} \times ng_{insert} \quad \text{A1}$$

Annex equation AI – Lambert-Beer Law

$$A = l \times \propto \times c \quad \text{A2}$$